Evaluation of Formulated Jatropha Oil as Cooling and Lubricating Cutting Fluids in Turning of AISI 1525 Steel Employing Taguchi-TOPSIS Technique

Rasaq Adebayo Kazeem[1,2] · Tien-Chien Jen[1] · Omolayo Michael Ikumapayi[3,4] · Esther Titilayo Akinlabi[5]

Abstract

This study examined the impact of cutting parameters and fluids on machining performance metrics, such as machine vibration rate and sound level, when turning AISI 1525 steel using tungsten carbide tools. Jatropha oil was used in two forms, minimum quantity lubrication and emulsion. Jatropha MQL was applied directly to the cutting region without any additives or water. Jatropha emulsion was formulated based on 4^4 full factorial techniques. Jatropha emulsion was formulated by mixing water, biocide, anticorrosive agent, antifoam agent, and emulsifier. The pH of the emulsified sample was used to determine the best formulation through optimization. Jatropha emulsion and Jatropha MQL were compared with their mineral oil equivalent during machining under Taguchi L_9 orthogonal array settings. The hardness of the workpiece was determined at every 5 mm diameter. Additionally, the microstructure of the workpiece was examined at 5 mm, 35 mm, and 70 mm diameters of the shaft. Multi-response optimization was performed using TOPSIS to determine optimal cutting parameters to minimize machine vibration rate and machine sound level. Results showed that jatropha MQL and jatropha emulsion reduced machine vibration rate drastically as compared to mineral oil counterparts. Jatropha MQL surpassed jatropha emulsion, mineral emulsion, and mineral MQL by 75.8%, 81.2%, and 90.5%, respectively. In terms of sound intensity, Jatropha oil MQL performed significantly better than other cooling and lubricating fluids based on general process parameter results. The hardness of the material increases as the diameter increases and it varies between 70.2 HBR and 150.4 HBR. Microstructural analysis showed the presence of pearlites and ferrites on the selected shaft diameters. Findings showed that the lowest machine vibration and machine sound values were achieved with experimental trial 1 such as spindle speed (355 rev/min), feed rate (0.10 mm/rev), and depth of cut (0.75 mm) in all cases of machining fluid. The optimal solutions of spindle speed, feed rate, and depth of cut were 355 rev/min, 0.10 mm/rev, and 0.75 mm; 355 rev/min, 0.15 mm/rev, and 1.00 mm for machine sound and machine vibrations, respectively.

✉ Rasaq Adebayo Kazeem
kazeemadebayo85@yahoo.com

1 Department of Mechanical Engineering Science, University of Johannesburg, Johannesburg 2006, South Africa

2 Department of Mechanical Engineering, University of Ibadan, Ibadan 200005, Nigeria

3 Department of Mechanical and Mechatronics Engineering, Afe Babalola University, Ado Ekiti 360101, Nigeria

4 Department of Mechanical and Industrial Engineering Technology, University of Johannesburg, Johannesburg 2028, South Africa

5 Department of Mechanical and Construction Engineering, Faculty of Engineering and Environment, Northumbria University, Newcastle NE1 8ST, UK

Abbreviation

MVR	Machine Vibration Rate
MSL	Machine Sound Level
SS	Spindle Speed
FR	Feed Rate
DOC	Depth of Cut
ANOVA	Analysis of Variance
DOE	Design of Experiment
MQL	Minimum Quantity Lubrication
HSS	High-Speed Steel
DOF	Degree of Freedom
MOS	Mean of Squares
SOS	Sum of Squares

1 Introduction

Machining is a manufacturing and prototype technique that removes unwanted components from a larger piece of material to obtain the desired shape [25]. This process is called subtractive manufacturing. Traditionally, highly specialized equipment is used for subtractive operations requiring metal cutting, such as lathe turning, drilling, milling, thread cutting, sawing, and gear cutting [26]. The machining performance is affected by various process parameters. Machining parameters consist of cutting tool, feed rate, spindle speed, machining time, depth of cut, etc. These parameters play a major role in machining which influences vibrations. Vibrations, commonly referred to as chatter, in manufacturing, are the varying motions of the cutting tool and the workpiece [32]. The vibrations cause significant waves on the machined material [50]. This affects common machining techniques like milling, turning, and drilling, as well as a common machining process like grinding. In machining, the vibration of the machine tool, cutting tool, and workpiece is a regular occurrence [9]. Vibration degrades product quality as well as the efficiency and lifespan of the machine tool and cutting tool [43]. Vibrations may increase to levels that adversely damage the machined surface accuracy. As far back as 1907, Frederick W. Taylor identified machining vibrations as the most inaccessible and intricate of all the difficulties confronting the machinist, an assessment that remains true today, as evidenced by several machining publications. Swain et al. [44] investigated the interaction between tool wear, surface roughness, and vibration during high-speed dry cutting employing the major input factor. Taguchi L27 DOE procedure was carried out using an uncoated carbide CNMG120408 tool and an alloy steel AISI 1040 workpiece. The results of the study revealed that the axial feed rate was the most important operational turning variable influencing surface roughness (91.97%). Rafighi [33, 34] investigated the effects of shallow cryogenic treatment on the surface properties and machining variables in AISI 4140 steel hard turning with a coated carbide insert. The influence of vibration, machining noise, and motor current on surface roughness was analyzed graphically. The findings revealed the relationship between machining noise, vibration, motor current, and surface roughness. The integrity of the machined surface degrades as the amount of the aforementioned responses increases. Kam and Şeremet [19] evaluated the vibration and surface roughness of an AISI 4140 (52HRc) steel workpiece during finish turning under wet and dry environments. The Taguchi method was employed in the statistical analysis of the experimental data. The measured and predicted data for the lowest vibration and surface roughness were 0.003463 gRMS

and 0.219 μm, and 0.003328 gRMS and 0.222 μm, respectively. Ghosh et al. [17] investigated the impact of process factors on cutting temperature and machine vibration during finish hard turning of AISI 4140 using coated carbide (CTC1135) cutting tools. RSM was used to plan the testing process. According to the statistical study, cutting speed had an insignificant impact on vibration, however, depth of cut (DOC) was shown to be highly significant on vibration frequency and cutting temperature. On top of that, Şahinoğlu and Rafighi [38] investigated the effect of cutting parameters on vibration, surface roughness, machine current, and sound intensity during AISI 4140 turning with coated carbide tools. The multiple linear regression method was used to generate statistical models. The results revealed that feed rate had the greatest influence on output characteristics, followed by DOC. All process parameters rise as DOC and feed rate increase, based on their experimental findings. Deshpande et al. [10] attempted to estimate the surface roughness process utilizing cutting variables, sound, cutting forces, and vibration in turning Inconel 718 with cryogenically treated and untreated carbide inserts. Şahinoğlu et al. [39], investigated the effect of cutting parameters on vibration, surface roughness, sound level, and motor current during turning tests of AISI 1040 workpieces at six distinct DOCs, four distinct feed rates, and cutting speeds without fluid. The full factorial design of experiment technique was applied. The results revealed that raising the feed rate raised the values of all output variables and that of all input variables, the feed rate was the most significant.

Also, Özbek and Saruhan [31] investigated the effects of cutting temperature, vibration, tool wear, and surface roughness in an environmentally friendly MQL turning of AISI D2 under MQL and dry circumstances. When contrasted to dry cutting, the results showed that cutting temperature, tool wear, and tool vibration amplitude were reduced by 25, 23, and 45%, respectively. These enhancements increased tool life by up to 267% and lowered the workpiece's surface roughness by 89%. Rao et al. [36] investigated surface roughness, tool wear, and workpiece vibration in drilling AISI 316 steel using cemented carbide tool inserts. The response parameters were predicted using ANN. The predicted results were contrasted to the experimental findings, and the percentage error was calculated. Akkuş and Yaka [3] sought to achieve excellent surface quality while using the least amount of energy during the turning operation of titanium 6Al-4V ELI alloy. The most important parameters in vibration, surface roughness, and energy consumption were determined to be feed rate. It was also discovered that as the frequency of vibration value increases, the energy consumption and surface roughness increase. Venkata Rao and Murthy [46] established statistical models to study the influence of cutting variables on root mean square vibration

and surface roughness in stainless steel boring. DOE claims that eighteen trials were carried out on AISI 316 stainless steel using PVD-coated carbide tools. The ANOVA method was used to determine important cutting parameters on root mean square vibration and surface roughness of the workpiece. The response variables were predicted using predictive models such as ANN, RSM, and SVM. In addition, Rafighi [33, 34] presented the results of an experimental investigation on the impacts of cutting parameters on machinability characteristics such as power consumption, surface roughness, machining force, and cutting sound in dry turning of Ti-6Al-4V titanium alloy employing CBN inserts. According to the results, increasing the machining sound increases the surface roughness and machining force while decreasing the power consumption. According to the desirability function, the best parameters for machining were 0.05 (mm) cutting depth, 0.04 (mm/rev) feed rate, and 60 (m/min) cutting speed. Bhogal et al. [6] studied the effect of cutting settings on surface roughness and tool vibration during EN-31 steel end milling. RSM was used to generate a statistical model for predicting tool vibration, surface finish, and tool wear using various cutting parameter combinations. The testing results revealed that feed rate was the most influential parameter determining surface finish, whereas cutting speed was the most influential factor controlling tool vibration. Ghani and Choudhury [15] investigated tool life, surface quality, and vibration when cutting nodular cast iron using a ceramic tool. Several cutting tests were performed to confirm the change in workpiece surface finish caused by increasing tool wear. When cutting nodular cast iron, the tool life of the alumina ceramic inserts was found to be insufficient. The highest tool life achieved in the speed range 364–685 m/min was just about 1.5 min. Sarma and Dixit [41] investigated the efficiency of a mixed oxide ceramic tool in air-cooled and dry gray cast iron turning. During the cutting process, surface roughness, tool wear, forces, and vibration were all investigated. Air-cooling was found to drastically minimize tool wear at high cutting speeds. Whereas dry turning worked poorly at higher cutting speeds, air-cooled turning gave a better surface finish.

Moreover, Ghorbani et al. [16] investigated the connection between design features, tool life, vibration, and fatigue strength. To achieve this goal, the vibration effect on tool wear was evaluated, which considers the shifting phase of vibration at various locations as well as forces on the tool's rear and rake faces. The findings of dynamic, static, and cutting tool tests with various fastening types, together with modeling outcomes, revealed an interaction between tool characteristics, tool life, and elastic system vibrations. Risbood et al. [37] evaluated the effectiveness of the generated neural network model through a series of experiments including wet and dry turning of mild steel bars with carbide and HSS tools. To estimate the

dimensional variation, the acceleration of radial vibration and the radial section of cutting force were used as feedback. D'Mello et al. [11] presented the results of a research investigation of cutting parameters, cutting tool vibrations, tool flank wear, and surface roughness characteristics when machining Ti-6Al-4V alloy. Turning experiments were carried out to investigate the variance in input and output variables. The findings demonstrated that cutting parameters had a strong influence on tool flank wear, and that as flank wear increased, so did surface finish. Cutting tool vibrations in the cutting speed direction correlated directly with surface roughness metrics. Bhuiyan and Choudhury [7] investigated surface finish and tool wear in turning Assab-705 steel by analyzing signals from vibrations. The investigation discovered that the RMS amplitude of vibration along all three axes varied with increasing cutting speed. The average frequency of diverse machine parts vibration was discovered to be between 0 Hz and 4.2 kHz, although the frequencies of different turning occurrences varied between 98 Hz and 42 kHz. Orhan et al. [30] evaluated the relationship between tool wear and vibration during AISI D3 steel end milling using an indexable CBN insert. It was discovered that the initial three multiplies of tooth passing frequency ($1 \times 2 \times 3$) provided the most precise data on tool wear. The findings demonstrated that there was no substantial rise in vibration amplitude until a flank wear value of 160 m was attained, after which the magnitude of the vibration substantially increased. Besides, Rao et al. [35] suggested a tool vibration-based methodology for evaluating surface roughness and tool wear when milling Ti-6Al-4 V alloy with a carbide-cement mill cutter. Measurements were carried out at optimum feed per tooth, cutting speed, and depth of cut levels, and findings from experiments for tool wear, tool vibration, and surface roughness were gathered until the flank wear equaled 0.3 mm. The grey prediction GM (1, N) system and support vector machine (SVM) optimization models were employed. The GM (1, N) optimization framework predicted surface roughness and tool wear with an average error of 0.7% and 3.03%, respectively, while the SVM was estimated with a mean error of 4.45% and 7.67%. Yi et al. [51] examined the machining of Ti-6A-4 V with a novel graphene-based cutting fluid experimentally. In a series of tests, three different forms of graphene oxide (GO) nanofluids with varying GO concentrations were used. Cutting force, tool wear, and vibration were measured while turning with novel nanofluids and conventional coolants. The cutting force was lowered by 50.83% when GO nanofluids were utilized, according to the data. When machining using GO nanofluids, the vibration was substantially reduced than when utilizing base fluids. Duan et al. [13] investigated performance characteristics such as surface roughness, workpiece/chip surface micromorphology, and

machining forces to determine the efficacy of six different nanofluid concentrations during MQL milling of grade 45 steel. In their experiment, cottonseed oil was blended with Al_2O_3 nanoparticles. According to the data, the lowest milling force was produced at a concentration of 0.2 wt% (Fx = 58 N and Fy = 12 N). The micromorphology of the workpiece/chip was outstanding, with a mass concentration of 0.5 wt%. In another study, Duan et al. [12] performed cutter element analysis and numerical simulation to calculate the cutting force of an integral end milling cutter. The instantaneous milling force model was developed using dry and MQL-assisted nano-cottonseed oil, with a twofold mechanism: shear on the cutter's rake face and plow cutting on the flank surface. The nanofluid MQL had average absolute errors of 13.3%, 2.3%, and 7.6% for determining milling forces in the x, y, and z axes. Nanofluid MQL milling forces were 21.4%, 17.7%, and 18.5% lower in the x, y, and z directions than dry milling forces. Zhenjing et al. [52] investigated the effects of helix angle, cavity shape, and milling cutter speed on the surrounding airflow field. The milling test of the nanofluid MQL cavity employed an Al_2O_3 nanofluid based on cottonseed oil, with a workpiece made of 7050 aluminum alloy. The authors reported that high rotational velocities of the milling cutter were responsible for the high velocity of the surrounding airflow field as well as the strong barrier.

Several scholars explored the relationship between vibrations and machining parameters based on the evaluated publications. Another major component that influences workpiece machinability is sound intensity. Some researchers have also reported the effect of machining settings on sound intensity. There have not been many studies that look at the connection between vegetable oil-based cutting fluids, and machine vibration and noise levels. As a result, this research looked into the application of jatropha oil as cutting fluids during the machining of AISI 1525 steel. Jatropha oil was utilized as an emulsion and lubricant. The performance of the two types of jatropha oil was compared with that of their mineral oil coequal. The effect of input factors such as feed rate, spindle speed, and depth of cut on output parameters such as machine vibration rate and machine sound level were investigated in this experimental investigation using tungsten carbide tools. The data from the experiment were analyzed using the Taguchi L_9 orthogonal array. The analysis of variance was used to identify the most effective parameters influencing response variables. However, the study used multiple linear regression equations to determine the response parameters based on the relationship between input and output characteristics. Machine vibration and sound values can be predicted with a high degree of accuracy using these equations. Furthermore, the effect of cutting parameters on output variables was investigated using response surface methodology. The TOPSIS approach was used to establish the optimum cutting settings as a result of this investigation.

2 Materials and Methods

2.1 Collection of Seeds and Oil Extraction

This study considered jatropha seeds which were purchased from a local market in Ibadan. The botanical name of the jatropha seed is *Jatropha cursas*. The study employed jatropha seeds because of their percentage oil content. According to Jonas et al. [18], the oil output in jatropha seed kernels varies from 38.7 to 45.8%. The seeds were purchased dried and manually cracked open using a pestle. Before grinding in the mechanical mill, more drying was done in the shade. Seed oil extraction was carried out chemically with hexane and following AOAC, [5] procedure. Afterward, distillation was conducted to separate the solvent from the jatropha oil. The phytochemical, physiochemical, and thermal characteristics of crude jatropha oil were studied. The properties' test results were published by Kazeem et al. [20]. Figure 1 shows the photographic views of the oil extraction process.

2.2 Formulation of Crude Oil Extracts into Cutting Fluids

This research considers two classes of cutting fluid (i) Neat oil cutting fluid and (ii) Emulsion cutting fluid. When machining, neat jatropha oil was applied straight without the use of water or additives [1, 4], in contrast, emulsion cutting fluid was developed by combining jatropha oil, filtered water, and additives. The additives utilized in the production of jatropha emulsion cutting fluid pose no risks to the ecosystem or machine personnel. The additives used to prepare the jatropha emulsion include (i) emulsifying agent, (ii) sodium molybdate, (iii) triazine, and (iv) silicones [22]. The emulsifying chemical aids in the formation of stable water and oil dispersions. It is a sodium sulfonate with a medium molecular weight that is linked to emulsion stabilization. It can be applied to soluble oil compositions intended for emulsification and cutting processes. The compositions of the emulsifier formulated are listed as follows: Sodium lauryl sulfate: 0.5 M; nitrosol: 0.5 M; sodium tripolyphosphate: 0.5 M; sulphonic acid: 0.5 M; calcium carbonate: 0.5 M; water: 5 L. Since sodium molybdate (Na_2MoO_4) is a non-oxidizing anodic inhibitor, it is utilized in the industry to suppress corrosion. The anticorrosion protection of carboxylate salt fluids is enhanced by the addition of sodium molybdate, which also greatly lowers the nitrite requirement of fluids inhibited with nitrite amine. Trizaine ($C_3H_3N_3$) prevents microbial contamination of

Fig. 1 Photographic views of the extraction process. (**a**) Dry jatropha seeds; (**b**) Milled jatropha seeds; (c) Milled seeds in the beaker before extraction; (**d**) Jatropha oil extraction; (**e**) Distillation process to separate hexane from extracted oil; and (**f**) Crude jatropha oil after extraction

fluid. It is a white crystalline solid with a melting point that ranges between 81 and 83 °C. Silicones, on the other hand, are used as active compounds in defoamers due to their poor water solubility and strong spreading capabilities. The effects of four variables were investigated at two levels (2^4 planning) using factorial planning indications. The four variables contain the previously mentioned additives, namely one emulsifying agent, one anticorrosion agent, one biocide, and one antifoam agent. Jatropha emulsions with 20% oil-to-water volumetric proportions were developed independently using 16 formulations derived from complete factorial approaches [8]. Tables 1 and 2 demonstrate the parameters of additives and levels used in the factorial design of the 2^4 full factorial designs, respectively.

Table 1 Factors and levels examined in the full factorial planning [20]

Factor	Symbol	Level	
		Maximum	Minimum
Emulsifying agent	A	12%	8.0%
Anticorrosive agent	B	2.0%	1.0%
Biocide	C	1.0%	0.5%
Antifoam agent	D	1.0%	0.5%

Table 2 Cutting fluids preliminary preparation volumes [20]

Exp. No	A (ml)	B (ml)	C (ml)	D (ml)	Water vol. (ml)
1	8.0	1.0	0.5	0.5	70.0
2	12.0	1.0	0.5	0.5	66.0
3	8.0	2.0	0.5	0.5	69.0
4	12.0	2.0	0.5	0.5	65.0
5	8.0	1.0	1.0	0.5	69.5
6	12.0	1.0	1.0	0.5	65.5
7	8.0	2.0	1.0	0.5	68.5
8	12.0	2.0	1.0	0.5	64.5
9	8.0	1.0	0.5	1.0	69.5
10	12.0	1.0	0.5	1.0	65.5
11	8.0	2.0	0.5	1.0	68.5
12	12.0	2.0	0.5	1.0	64.5
13	8.0	1.0	1.0	1.0	69.0
14	12.0	1.0	1.0	1.0	65.0
15	8.0	2.0	1.0	1.0	68.0
16	12.0	2.0	1.0	1.0	64.0

Fig. 2 Complete Formulation Process of Jatropha Emulsion Cutting Fluid

2.3 Preparation and Characterization of Emulsion Metal Cutting Fluids

Each test, as shown in Table 2, was made by first combining oil and filtered water, and then adding the four additives. The aggregate volume of each experiment was 100 ml. Figure 2 depicts the preliminary jatropha emulsion cutting fluid development procedure. The goal was to investigate the ideal makeup for these mixtures as well as the efficacy of the modifications. This combination was made with the help of a magnetic stirrer at a speed of 800 rpm (see Fig. 3). For 10 min, the combination was examined at room temperature [24]. The stability test, percentage of foam generated, and pH were used to evaluate the jatropha emulsion.

2.3.1 Determination of Stability of Jatropha Emulsion

The phase separation stability of jatropha emulsion (tests 1–16) was physically examined for one day at room

Fig. 3 Mixing Process of Jatropha Emulsion Formulation

temperature in 100 ml measuring cylinders (with 1 ml partitions) [29]. The findings are expressed as a volumetric percentage of water separated from the original mixture (% vol. water).

2.3.2 Determination of Foaming of Jatropha Emulsion

A foaming test was carried out on the 16 assays after the 24-h stability test. Formulations were diluted 20:1 in water, and then 50 ml of each dilute formulation was added to a 100 ml measuring cylinder. The cylinder was shaken manually several times over one minute. Foam heights were recorded after 5 min of cylinder shakes.

2.3.3 Determination of pH of Jatropha Emulsion

The pH of the fluid indicates its state. A reduction in the pH value implies a decline in the cutting fluid's functionality. A pH level that is extremely high or low can be dangerous to human operators and cause waste disposal issues. The pH value was estimated using a digital pH gauge. The pH value results were evaluated statistically using the design of experiment software. For prediction of the response, Y, which incorporates all factors as well as the most effective manner the elements interact, the software utilized for the analysis employs a second-degree polynomial, calculated by Eq. 1, [24, 29].

$$y = \beta_o + \sum \beta_i x_i + \sum \beta_{ii} x_i^2 + \sum \beta_{ij} x_i x_j, \tag{1}$$

where β_o is constant, βi and βij are coefficients of ij, xi represents independent variables, and xij denotes the interactions thereof [24]. The ideal parameters found were used to generate the final emulsion employed in this study for machining.

2.4 Workpiece Procurement

In this research, AISI 1525 steel with dimensions of 1200 mm × 85 mm was purchased from a scrap yard in Nigeria. As illustrated in Fig. 4, the workpiece's length was decreased to 140 mm and its diameter reduced to 75 mm.

2.4.1 Characterization of Workpiece

To understand and use AISI 1525 steel, the chemical and physical characteristics or properties of the workpiece were determined. These properties were determined to identify the constituents that made up a workpiece and at the same time to describe them. The tensile, hardness, and chemical analyses of the workpiece sample were carried out before machining. Tensile tests on the specimens were performed using a computerized Instron electromechanical universal tensile testing machine. The system consisted of software that processed the incoming signal and instructed the machine on how to do the test, which consisted of tugging the specimen in opposing directions until it fractured [1]. The hardness of AISI 1525 steel was evaluated at fourteen different locations to validate improvement in their mechanical properties. The hardness value was measured at every 5 mm diameter decrease of the workpiece. The hardness is calculated based on three factors: the applied load, the diameter of the ball, and the diameter of the indenter. In this paper, the corresponding hardness values were calculated using Eq. (2).

$$BHN = \frac{2P}{\pi d_i \left[D_b - \sqrt{D_b^2 - d_i^2} \right]}, \tag{2}$$

where P = Load applied (500 kgf), d_i = Diameter of indentation (10 mm), D_b = Diameter of the ball (mm).

The microstructural examination was carried out on the workpiece to ascertain whether there were microstructural deformations or microstructural changes in the workpiece before machining. This was observed at three different locations of the workpiece, i.e., 70 mm, 35 mm, and 5 mm diameters of the workpiece. The microstructure was carried out with a metallurgical microscope. The magnification employed was 200X [21].

Fig. 4 Some of the AISI 1525 steel used for the machining

2.5 Cutting Tool and Machining Experiments

Turning operation was carried out on an AJAX conventional machine with a range of spindle speed (16 -2000 rpm), feed range (0.06–0.73 mm/rev), 4-way tool post, and three jaw-dependent chuck. For the turning process, tungsten carbide inserts tools (tool holder model: MCLNR2020K12, insert model: CNMG12040408, insert size: 12, shank length: 100 mm, and insert shape: triangular) were utilized [20]. The cutting insert and tool holder used for machining are shown in Fig. 5. Both wet cooling and MQL techniques were adopted for the application of cutting fluids. Jatropha MQL and mineral MQL were supplied as mist at 2.3 mL/h to the cutting interface. Taguchi L_9 orthogonal array was employed to plan the experiments. As a result, a total of nine machining attempts were conducted. Table 3 shows the cutting parameters and levels that have a major effect on the responses (machine vibration rate and machine sound level).

2.6 Measuring Equipment

During the machining process, vibrations are unavoidable. A vibration meter (Lutron Vibration Meter VB8206SD) was used to measure machine vibration under various cutting scenarios. The vibration meter probe was put near the spindle, next to the machine's headstock. The meter measures velocity, displacement, and acceleration, although the measurement for this investigation was measured in terms of acceleration (m/s^2). It is capable of recording the least and maximum spindle vibration over time (in the form of a sensor). However, the noise from the machine was measured using a sound level meter (Testo815) and a sound recording and analysis software tool named Cool Edit. The software application was launched, and the noise recording interface was set to 96,000 samples per second, 32-bit (float) resolution, and stereo channels. The laptop was situated approximately 1.2 m from the machine. Figure 6 (a) and (b) shows pictorial views of the measuring devices.

2.7 Optimization of Cutting Parameters Using TOPSIS

The Taguchi method is well known for its ease of use and efficacy in variable optimization; however, it is limited to single-objective optimization [2]. However, to solve the issue of optimization issues with multiple objectives and deliver effective solutions, TOPSIS integration with Taguchi DOE has grown in popularity. This integration provides a solution by using TOPSIS to simplify the multi-objective problem into a single-objective problem [53]. TOPSIS can be used to identify the optimum values depending on the transformed single output value, allowing for efficient decision-making in optimization with
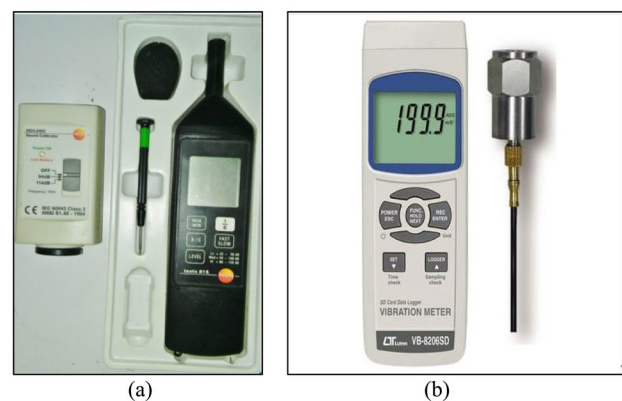

Fig. 5 Tool holder and cutting inserts

Table 3 Cutting parameters and their levels [22]

Exp. No	v (rev/min)	f mm/rev(	a_p (mm)
1	355	0.10	0.75
2	355	0.15	1.00
3	355	0.20	1.25
4	500	0.10	1.00
5	500	0.15	1.25
6	500	0.20	0.75
7	710	0.10	1.25
8	710	0.15	0.75
9	710	0.20	1.00

Fig. 6 Measuring Equipment (**a**) Sound Level Meter (**b**) Vibration Meter

multiple goals. The Euclidean measurements of every possible solution from the perfect and anti-perfect solutions are calculated in this optimization approach. The best option should be placed closest to the perfect solution and farthest away from the anti-perfect solution in this strategy. Its use requires the following steps:

Step I—Obtained output data were first normalized using Eq. (3) to determine the corresponding decision matrix.

$$z_{ij} = \frac{x_{ij}}{\overline{X}} \tag{3}$$

where $\overline{X} = \sqrt{\sum_{j=1}^{n} x_{ij}^2}$

Step II—Develop a weighted normalized decision matrix. The weight is applied to each element of the output. For this study, two output variables (M_V and M_{SL}) were equally relevant, hence equal weight was assigned to each of them. As a result, each output variable weighs 0.5 (50% weightage each), which is multiplied by the normalized matrix value given by Eq. (4).

$$U_{ij} = w_i \times z_{ij} \tag{4}$$

Step III—Identify the ideal (F^+) and anti-ideal (F^-) solutions using Eqs. (5) and (6), respectively.

$$F^+ = \left\{ u_1^+, u_2^+, ...u_i^+, ...u_n^+ \right\} \tag{5}$$

$$F^- = \left\{ u_1^-, u_2^-, ...u_i^-, ...u_n^- \right\}, \tag{6}$$

where u_i^+ and u_i^- are the best value, respectively, the worst value for the ith criterion among all alternatives.

Step IV—Using Eq. (7), find the n-dimensional Euclidean separation between each potential outcome and the ideal outcome.

$$P_j^+ = \sqrt{\sum_{i=1}^{k} \left(u_{ij} - u_i^+ \right)^2}, \quad j = \frac{1}{n} \tag{7}$$

Step V—Determine the distance in n-dimensions between each potential solution and the negative ideal solution using Eq. (8)

$$P_j^- = \sqrt{\sum_{i=1}^{k} \left(u_{ij} - u_i^- \right)^2}, \quad j = \frac{1}{n} \tag{8}$$

Step VI—Calculate the relative closeness (the degree to which the solution is closest to the ideal) using Eq. (9)

$$Q_j = \frac{P_j^-}{P_j^+ + P_j^-}, \quad j = \frac{1}{n} \tag{9}$$

The maximum value of Qj rank is 1 and other values are assigned appropriately. The relative closeness and rank are established using the preceding procedures.

3 Results and Discussion

This section is divided into five phases (i) Evaluation of vegetable oil emulsion formulation, (ii) evaluation of material properties, (iii) experimental examination of process parameters, (iv) optimization of process parameters for machine vibration rate and machine sound level, and (v) Statistical analysis. The following sections contain all of the necessary details.

3.1 Evaluation of Vegetable Oil Emulsion Formulation

3.1.1 Evaluation of Stability of Jatropha Emulsion

Concerning the stability tests, the 20% oil in water emulsions were analyzed, assays 9, 10, 12, 14, and 16 could remain stable for jatropha emulsion after 24 h; and the other assays presented between 89 and 99% of water separation.

3.1.2 Evaluation of Foaming of Jatropha Emulsion

Foaming subsided within one minute in all formulations after the initial reading. The foaming value in jatropha emulsion ranges from 1.1 to 2.5 ml. Jatropha emulsion showed an encouraging result by producing a foaming height of 1.1 (minimum) and 2.5 (maximum). The least foaming height was achieved by assay 10. Jatropha emulsion tends to suppress the action of emulsifier. This may be due to some natural compounds contained in the jatropha oil. Emulsion metal cutting fluids are regarded to be of good performance when they produce a lesser foam height.

3.1.3 Evaluation of pH of Jatropha Emulsion

Cutting fluid microbiological contamination occurs in acidic rather than alkaline media. The pH values of 8.0 and above will not corrode metals during machining and such cutting fluids will be skin friendly to machine operators using it. The increase in pH values suggests that the fluid is more resistant to microbial infection. The pH values ranged from 9.6 to 9.8 for all the assays examined and these fall within

the acceptable pH for typical cutting fluid formulations. Table 4 shows the pH of 16 preliminary formulations that were examined.

3.2 Optimization of Additives for Formulation of Jatropha Oil Emulsions

Due to the sensitivity of the pH of the cutting fluid, the study decided to optimize the additives used for jatropha emulsion with the parameter. The pH values were statistically evaluated using the design of experiment software. The ideal additive values were employed to produce the final stage of jatropha oil emulsion. The main effect plot was obtained for the jatropha emulsion. The result was further analyzed using ANOVA and regression equation. However, the main effect plot for 20 percent oil content analysis is depicted in Fig. 7. The most favorable conditions considered for the pH are 12.0 ml of emulsifier (level 2), 1.0 ml of anticorrosive agent (level 1), 1.0 ml of biocide (level 2), and 0.5 ml of antifoam agent (level 1). The ANOVA analysis for the pH is presented in Table 5. It shows the impact of each input factor for 20 percent oil content as an emulsifier (85.26316%), anticorrosive agent (4.210526%), biocide (0.421053%), and antifoam agent (1.052632%). The result has proven that emulsifying agent (85.26%) is a determinant for the pH of the jatropha emulsion formulation. The impact of anticorrosive agents, antifoam agents, and biocide is less significant. This analysis specifies a confidence level of 95%. The pH model for jatropha emulsion is given by Eq. (10).

$$pH = 9.4312 + 0.02812A - 0.0125B - 0.0250C - 0.0250D, \tag{10}$$

where $A = 12.0$ ml, $B = 1.0$ ml, $C = 0.5$ ml, and $D = 0.5$ ml.

$$R^2 = 88.42\% \quad \text{and} \quad R^2(adj) = 84.21\%$$

Table 4 pH values of 16 assays of jatropha emulsion

Assay No	1	2	3	4	5	6	7	8	9	10	11	12	13	14	15	16
pH	9.6	9.8	9.6	9.7	9.6	9.7	9.6	9.7	9.6	9.7	9.6	9.7	9.6	9.7	9.6	9.7

Fig. 7 Main effect plot for jatropha oil emulsion
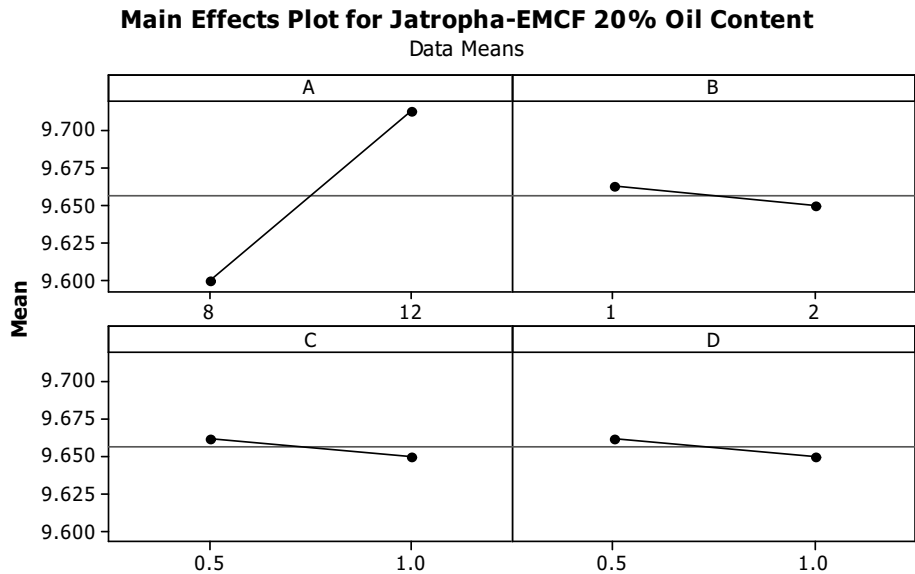
Table 5 ANOVA for pH of jatropha oil emulsion

Oil sample	Factor	DOF	SOS	MS	F	P%
Jatropha 20% oil content	A (ml)	1	0.050625	0.050625	103.6047	85.26316
	B (ml)	1	0.0025	0.0025	5.116279	4.210526
	C (ml)	1	0.00025	0.00025	0.511628	0.421053
	D (ml)	1	0.000625	0.000625	1.27907	1.052632
	Error	11	0.005375	0.000489		9.052632
	Total	15	0.059375	0.003958		100

Table 6 Confirmation test percentage error

Sample pH	Calculated value	Experiment value	Percentage error
Jatropha Emulsion	9.73	9.8	0.0071

3.3 Confirmation Test Percentage Error

Experimentation was carried out using the optimized input variables that were acquired. This was performed to verify the regression models used for pH analysis. The experiment findings were juxtaposed to the optimal values, and the percentage errors were computed, as shown in Table 6. The pH error between experimental results and the mathematical model was calculated to be 0.0071 (0.71%). As a result, established mathematical models relate the relationship between input and output characteristics with high degrees of accuracy. After verification, the ideal additive ratios were employed to produce the final jatropha emulsion cutting fluid used for experiments. Kazeem et al. [20] reported on the qualities of the formulated jatropha emulsion.

3.4 Evaluation of Material Properties

The chemical and physical characteristics of AISI 1525 steel are shown in Tables 7 and 8, respectively. The hardness at every 5 mm diameter of the shaft is shown in Fig. 8. The hardness increases as the diameter increases from 5 to 70 mm diameter of the shaft. The hardness has increased from 70.20 to 150.40 mm. The average hardness of the steel is 110.05 mm.

The microstructural images of the workpiece at 200X magnifications are exhibited in Fig. 9 (a–f). On the surface of the micrograph, pearlite and ferrite particles can be observed, which are randomly orientated and have uniform

Table 7 Chemical properties of AISI 1525 steel material

Element	% Composition
Fe	97.9285
Ti	0.0395
C	0.2505
Mn	1.2340
S	0.0235
Al	0.0120
Cr	0.1135
P	0.0135
Ni	0.1155
Nb	0.0001
Cu	0.0480
Si	0.2215

Table 8 Mechanical properties of AISI 1525 steel

Properties	Values
Energy at break	47.35634 J
Energy at maximum tensile stress	31.24909 J
Elastic modulus	35,106.19 MPa
Yield strength	7599.34 MPa
Tensile strength	604.74 MPa

distribution in the material. The steel microstructure at 5 mm diameter has both white and black patches. The white area is the ferrite phase, and the black area is the pearlite phase. It features a clear grain boundary and a higher ferrite phase than pearlite. The steel microstructure at 35 mm diameter reveals equal proportions of pearlite and ferrite. There are small and cluster phases of ferrite and pearlite at 70 mm in diameter. The grains are closer together, and this steel has a greater hardness value because the grain boundaries are closer together when compared to 35 mm and 5 mm diameters. Finer grain sizes at 70 mm diameter may improve material toughness and strength [14, 27] and [21]). Finer grain sizes, according to Yan et al. [49], and Koushki et al. [23], give improved grain boundaries, increase deformation resistance, and restrict dislocation migration. These are some of the aspects that influence steel's mechanical performance. The occurrence of pearlites at 70 mm diameter vs 5 mm and 35 mm diameters could also account for the increased hardness, as pearlites are hard and robust, but ferrite is soft [21].

3.5 Experimental Investigation of Process Parameters

Table 9 displays the experimental findings of cutting AISI 1525 steel with a tungsten carbide tool. The machine vibration and sound readings for each of the four cutting environments are displayed.

The vibrations cause waves to form on the machined surface. Machine vibration left uncontrolled may increase wear rates (i.e., lower tool life) and damage equipment [43, 45]. Vibration can make noise, cause safety issues, and degrade factory working conditions. Vibration can cause machinery to consume too much electricity and harm product quality [28]. Furthermore, the use of cooling conditions considerably reduces machine vibration during turning operations. As a result, in this investigation, machine vibration was regarded as a crucial machining index. Figure 10 depicts the effect of machine characteristics and cooling conditions on machine vibration. Jatropha-based oils provided lower machine vibration values than mineral cutting fluids. The machine vibration rate of emulsion cutting fluids was found to be between 2.10 and 29.20 ms^{-2} for jatropha oil and 7.91 and 42.9 ms^{-2} for mineral oil. Machine vibration values for
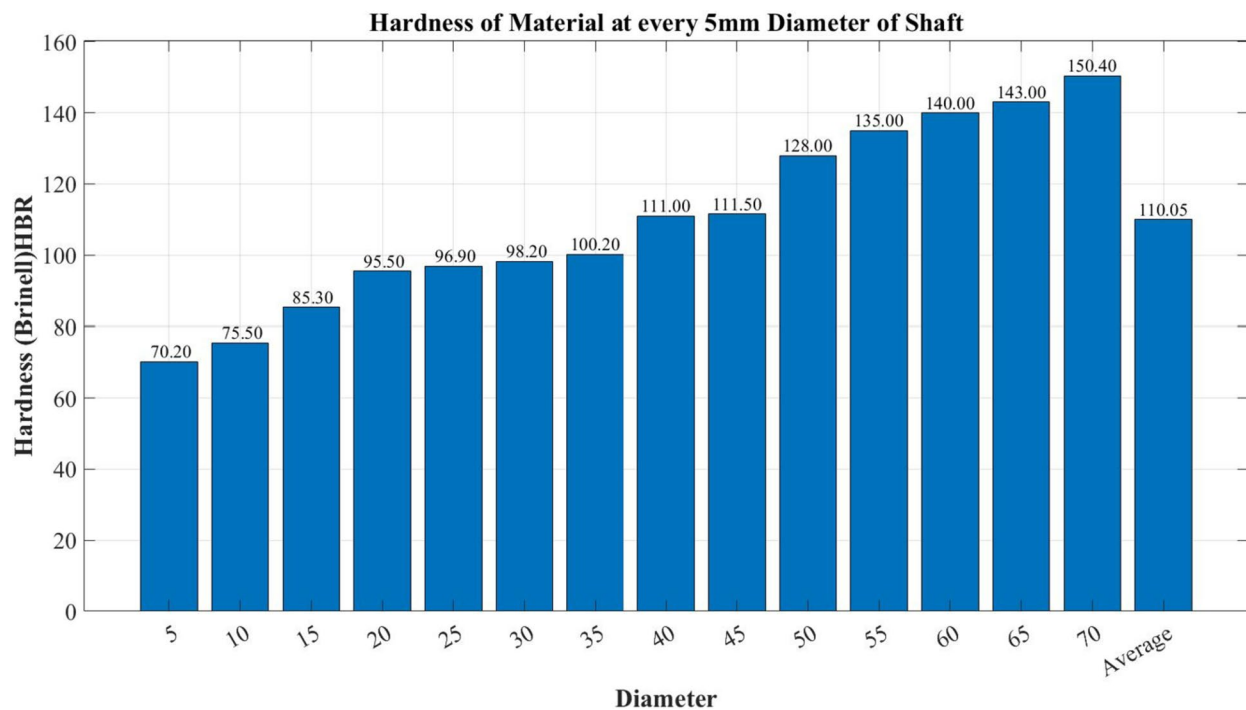
Fig. 8 Hardness of material at every 5 mm diameter of AISI 1525 steel

MQL machining range from 1.80 to 13.96 ms^{-2} and from 5.12 to 72.02 ms^{-2}, respectively. In both examples of cutting fluids, jatropha oil had the lowest machine vibration values, whereas mineral oil had the highest. In general, the average and standard deviation values of jatropha emulsion, jatropha MQL, mineral emulsion, and mineral MQL are 18.6 ± 10.5, 4.5 ± 3.81, 23.9 ± 10.7, and 47.14 ± 31.25 ms^{-2}, respectively. Lower machine vibration rates, it is believed, result in better machining. In general, vegetable oil-based cutting fluid outperformed mineral oil. When compared to mineral oil emulsion and straight oil, the jatropha emulsion and neat oils significantly reduced the machine vibration rate. Jatropha MQL surpassed jatropha emulsion, mineral emulsion, and mineral MQL by 75.8%, 81.2%, and 90.5%, respectively. Moreover, the emulsion jatropha outperformed mineral emulsion and mineral MQL by 28.5% and 60.5%, respectively. At a spindle speed of 355 rev/min and feed rate of 0.10 mm/rev, a decrease in depth of cut improved the machine vibration rate during the MQL turning of AISI 1525 steel with jatropha oil. Similar results have been reported in Şahinoğlu and Rafighi [38] and Ghani and Choudhury [15].

One of the variables leading to industrial pollution is noise. The noise produced by materials during machining operations is linked with a range of distinct noise sources, and each noise signal has varying temporal and frequency domain properties [48]. Noise in actual work is mostly caused by machine tool noise and cutting noise caused by dynamic interaction between the material and the tool

[47]. The machine tool's interior structure is the source of the noise. Noise generators in the machine tool include gears, bearings, and motors. However, high-intensity noise induced during high-speed cutting can affect processing efficiency, workpiece quality, and processing accuracy. The results obtained for machine sound level by employing four machining oils, namely, jatropha emulsion, mineral emulsion, jatropha MQL, and mineral MQL are presented in Table 9. From the analysis, machine noise fell within the ranges of 82–107 dB, 85.7–111.1 dB, 80.9–99.3 dB, and 86.1–116.6 dB for jatropha emulsion, mineral emulsion, jatropha MQL, and mineral MQL, respectively. The average and standard deviation values were 99.32 ± 8.86, 97.2 ± 11.6, 90.2 ± 6.28 an,d 104.8 ± 11.28 for jatropha emulsion, mineral emulsion, jatropha MQL, and mineral MQL, respectively. The desired outcome was often captured with lower machine sound intensity. In terms of sound intensity, Jatropha oil MQL performed significantly better than other cooling and lubricating fluids based on general process parameter results. Findings showed that the lowest machine sound level in all cases of machining fluid was achieved with experimental trial 1 such as spindle speed (355 rev/min), feed rate (0.10 mm/rev), and depth of cut (0.75 mm). This could be because the cutting tool was still fresh at the time, and as such plays an essential role in decreasing noise pressure levels and the effect of noise on the processing environment. Also, the experimental trial number experienced reduced noise
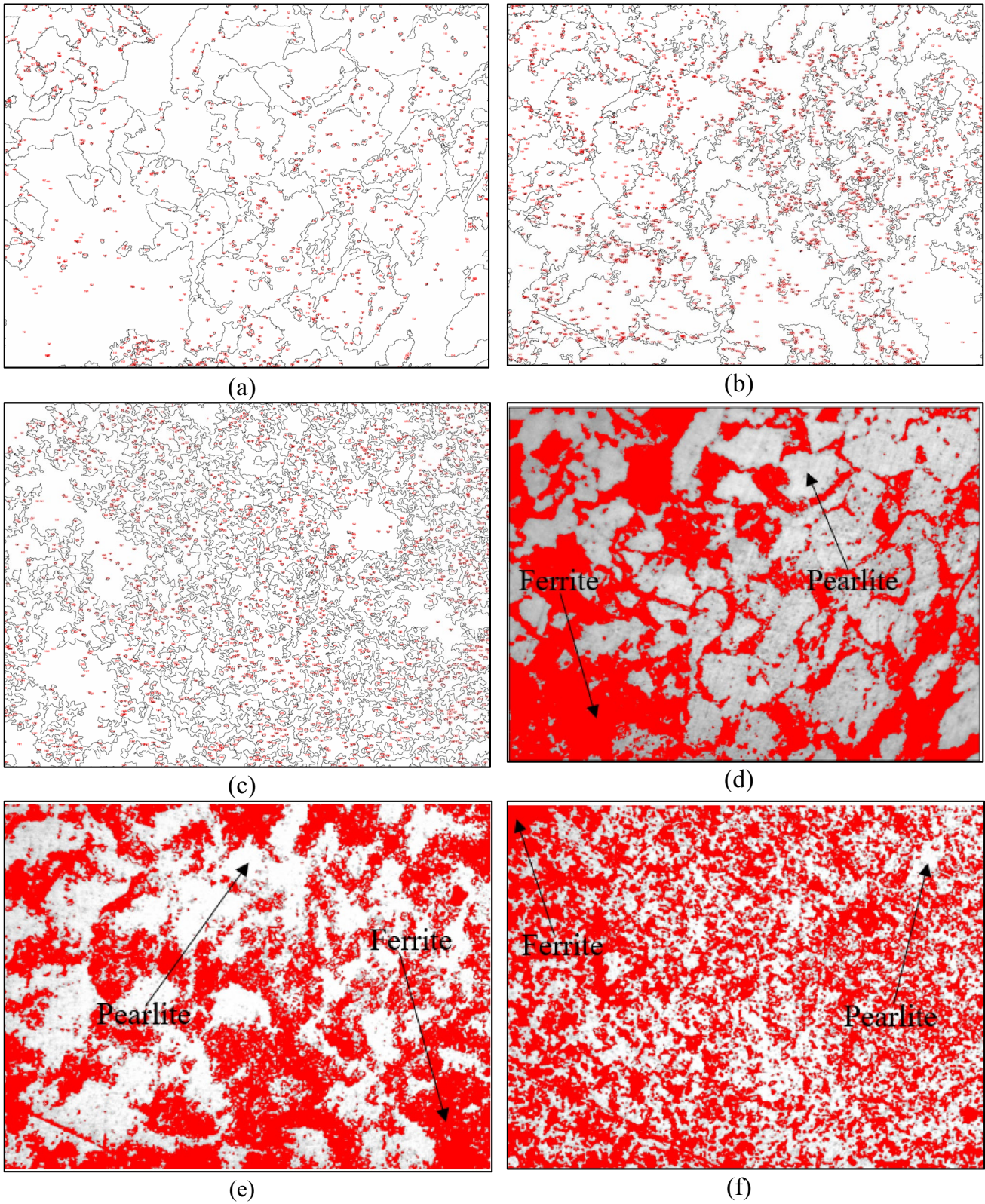
Fig. 9 (**a**) Microstructure of the steel at 5 mm diameter (**b**) Drawing of the steel at 5 mm (**c**) Microstructure of the steel at 35 mm diameter (**d**) Drawing of the steel at 35 mm (**e**) Microstructure of the at 70 mm diameter (**f**) Drawing of the steel at 70 mm

Table 9 Experimental observations of various cooling and lubricating fluids

Exp. No	Jatropha oil emulsion		Mineral oil emulsion		Jatropha oil MQL		Mineral oil MQL	
	MSL (dB)	MVR (ms^{-2})	MSL (dB)	MVR (ms^{-2})	MSL (dB)	MVR (ms^{-2})	MSL (dB)	MVR (ms^{-2})
1	82.0	2.10	85.7	27.03	80.9	1.80	86.1	5.12
2	88.6	6.81	85.9	7.91	83.6	2.70	93.8	10.6
3	95.1	7.99	86.0	28.7	84.0	2.68	104.6	55.5
4	101.7	18.88	85.7	15.5	93.9	4.33	116.6	82.7
5	107.0	26.73	95.5	42.9	97.0	13.96	114.4	72.02
6	105.9	19.56	108.8	21.4	89.8	2.35	112.1	81.9
7	105.1	29.20	106.9	29.2	99.3	6.49	111.4	52.6
8	105.9	27.02	111.1	12.9	91.8	2.95	92.0	8.9
9	102.6	29.07	109.0	29.95	91.6	3.26	112.2	54.9

Fig. 10 Effect of different cooling and lubricating fluids on machine vibration rate
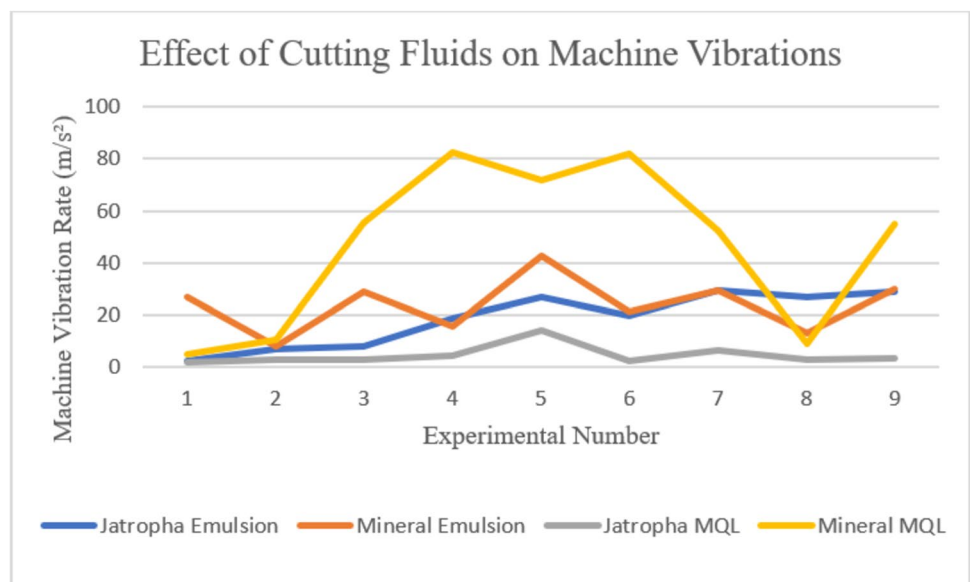
Fig. 11 Effect of different cooling and lubricating fluids on machine sound level
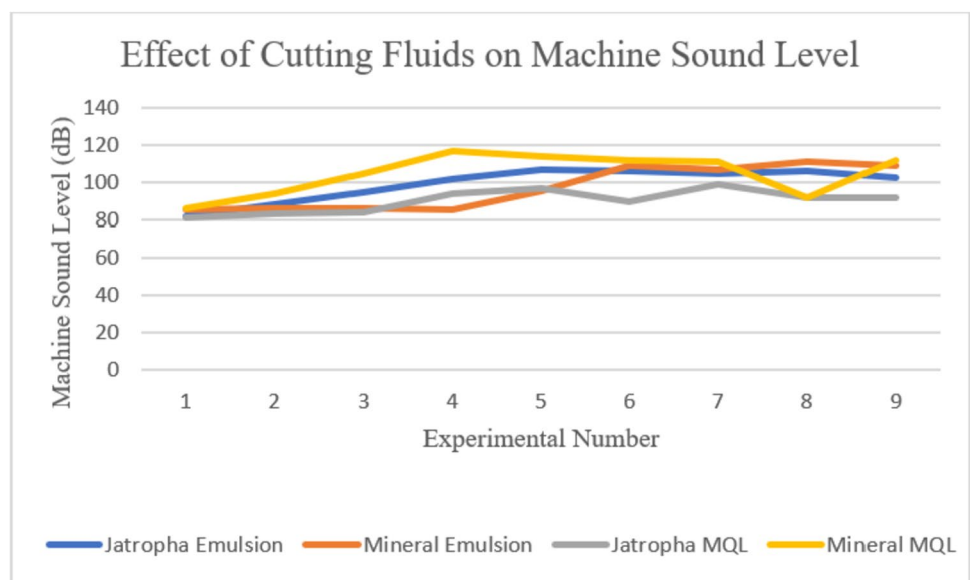
intensity but not as low as experiment 1 (see Fig. 11). The values obtained may have been influenced by the condition of the cutting tool. The precision and efficiency of workpiece processing are directly impacted by the status of the tool; thus, it is imperative to keep an eye on it during the machining process. Furthermore, damage to the machine tool and machined surface results from the continuous operation of a failed tool. At the top spindle speed of 710 rev/min, the sound level increased for all machining fluids except for the case of mineral oil MQL. The noise performance of jatropha MQL exceeded jatropha oil emulsion, mineral oil emulsion, and mineral MQL by 9.2%, 7.2%, and 13.9%, respectively. In terms of overall performance, jatropha MQL reduced the frictional force during machining of AISI 1525 steel which in turn lowered machining noise and vibrations. Jatropha emulsion as regard machine sound level competed with mineral oil emulsion to an acceptable extent as the conventional fluid hardly outdo it by approximately 22%. The behavior experienced by jatropha oil is in rapport with Sen et al. [42], and Sani et al. [40]. This is also in accordance with Lawal et al. [24]. The order of effectiveness of lubricating oil is jatropha MQL, jatropha emulsion, mineral emulsion, and mineral MQL. This demonstrates that when compared to mineral oil samples, jatropha oil has more fluidity and a faster cooling capability. The inclusion of water and additives distinguishes jatropha oil emulsion from its straight application for the least quantity of lubrication. Its effectiveness was diminished when water and additives were diluted with crude jatropha oil. Jatropha oil's triglyceride composition offers benefits that make it an attractive lubricant. Jatropha oil's long, polar fatty acid chains produced powerful lubricant coatings that interact well with metallic surfaces to lower wear and friction. Strong intermolecular connections resulting from the usage of jatropha oil

provide a more stable viscosity or high viscosity coefficient, that is also resistant to temperature variations.

3.6 Evaluation of TOPSIS Analysis

The TOPSIS method was used to obtain the ranking of the test combinations concerning their general effectiveness after establishing the experimental findings for machine vibration rate and machine sound level. First, the problem's decision matrix was created, as shown in Table 9. With the aid of Eq. (3), the decision matrix's entries are further normalized to make the values obtained from the various output parameter scales comparable. For machine sound level and machine vibration rate, respectively, Tables 10 and 11 display the normalized decision matrix. Weighted normalized decision matrices are computed using Eq. (4) after normalization and are also displayed in Tables 10 and 11, respectively. The positive (F^+) and negative (F^-) ideal reference points were calculated using Eqs. (5) and (6) and are shown in the lower part of Tables 10 and 11 after the weighted normalized decision matrix was established. The Euclidian distance between each alternative and P_j^+ and P_j^- was then calculated using Eqs. 7 and 8, respectively. The P_j^+ and P_j^- results are shown in Table 12 for machine sound level and Table 13 for machine vibration rate, respectively [9]. Finally, the closeness coefficient (Q_j) is calculated using Eq. (9) and is provided in Tables 12 and 13, for machine sound level and machine vibration, respectively. For the two process parameters, the experiment rankings are displayed in the very right column of Tables 12 and 13.

Table 10 Normalized and weighted normalized decision matrix for machine sound level

Exp. No	Normalized decision matrix for MSL (dB)					Weighted normalized decision matrix for MSL (dB)			
	Jatropha emul	Mineral emul	Jatropha MQL	Mineral MQL		Jatropha emul	Mineral emul	Jatropha MQL	Mineral MQL
E1	0.27423	0.29211	0.2983	0.2725		0.068558	0.07303	0.074571	0.06811
E2	0.29630	0.2928	0.3082	0.2968		0.074076	0.07320	0.07706	0.07421
E3	0.31804	0.2931	0.3097	0.3310		0.07951	0.07328	0.077429	0.08275
E4	0.34011	0.29211	0.3462	0.3690		0.085028	0.07303	0.086555	0.09224
E5	0.35784	0.3255	0.3577	0.3620		0.089459	0.08139	0.089412	0.09050
E6	0.35416	0.3709	0.33110	0.3547		0.08854	0.09271	0.082775	0.08868
E7	0.35148	0.3644	0.3661	0.3525		0.087871	0.09109	0.091532	0.08813
E8	0.35416	0.3787	0.3385	0.29113		0.08854	0.09467	0.084619	0.07278
E9	0.34312	0.3715	0.3377	0.3551		0.085781	0.09288	0.084434	0.08876
					F^+	0.068558	0.07303	0.074571	0.06811
					F^-	0.089459	0.09467	0.091532	0.09224

Table 11 Normalized and weighted normalized decision matrix for machine vibration rate

Exp. No	Normalized decision matrix for MVR (ms^{-2})					Weighted normalized decision matrix for MVR (ms^{-2})			
	Jatropha emul	Mineral emul	Jatropha MQL	Mineral MQL		Jatropha emul	Mineral emul	Jatropha MQL	Mineral MQL
E1	0.0332	0.3469	0.1042	0.0307		0.008305	0.08672	0.026054	0.00768
E2	0.1077	0.1015	0.1563	0.0636		0.026933	0.02538	0.039081	0.01589
E3	0.1264	0.3683	0.1552	0.3328		0.031599	0.09208	0.038792	0.08320
E4	0.2987	0.1989	0.2507	0.4959		0.074668	0.04973	0.062674	0.12397
E5	0.4229	0.5506	0.8082	0.4319		0.105713	0.13764	0.202063	0.10796
E6	0.3094	0.2746	0.1361	0.4911		0.077357	0.06866	0.034015	0.12277
E7	0.4619	0.3747	0.3758	0.3154		0.115482	0.09369	0.093939	0.07885
E8	0.4274	0.1656	0.1708	0.0534		0.10686	0.04139	0.0427	0.01334
E9	0.4599	0.3844	0.1888	0.3292		0.114967	0.09609	0.047187	0.08230
					F^{+}	0.008305	0.02538	0.026054	0.00768
					F^{-}	0.115482	0.13764	0.202063	0.12397

Table 12 Performance index of machine sound level by TOPSIS

Exp. No	$P_j{}^{+}$	$P_j{}^{-}$	Q_j	rk (A)
E1	0.00033	0.03952	0.99166	1
E2	0.00859	0.03511	0.80343	2
E3	0.01850	0.02908	0.61111	3
E4	0.03158	0.02265	0.41766	4
E5	0.03504	0.01357	0.27919	6
E6	0.03574	0.00970	0.21344	7
E7	0.03725	0.00568	0.13229	9
E8	0.03147	0.02067	0.39645	5
E9	0.03485	0.00890	0.20345	8

Table 13 Performance index of machine vibration rate by TOPSIS

Exp. No	$P_j{}^{+}$	$P_j{}^{-}$	Q_j	rk (A)
E1	0.05686	0.14526	0.71870	2
E2	0.02616	0.16336	0.86197	1
E3	0.10113	0.08056	0.44341	6
E4	0.13173	0.08099	0.38074	9
E5	0.12108	0.07770	0.39088	7
E6	0.12849	0.08117	0.38716	8
E7	0.08885	0.13243	0.59848	3
E8	0.12954	0.11320	0.46635	5
E9	0.09815	0.08723	0.47056	4

Table 14 Main effects on mean relative closeness for machine sound level

Turning parameter	TOPSIS average by factor level				
	Level 1	Level 2	Level 3	Delta	Rank
SS (rev/min)	0.8021	0.3034	0.2441	0.5580	1
FR (mm/rev)	0.5139	0.4930	0.3427	0.1712	3
DOC (mm)	0.5339	0.4748	0.3409	0.1930	2

Table 15 Main effects on mean relative closeness for machine vibration rate

Turning parameter	TOPSIS average by factor level				
	Level 1	Level 2	Level 3	Delta	Rank
SS (rev/min)	0.6747	0.3863	0.5118	0.2884	1
FR (mm/rev)	0.5660	0.5731	0.4337	0.1394	2
DOC (mm)	0.5241	0.5711	0.4776	0.0935	3

3.7 Optimization of Response Variables Using TOPSIS Technique

From Tables 12 and 13, the results of experiment 1 and experiment 2 showed that the machine sound level and vibration rate had the maximum relative closeness, at 0.99166 and 0.86197, respectively. These values are close to the ideal value of 1. The mean responses, which are displayed in Tables 14 and 15 for machine sound level and machine vibration rate, were developed to verify the ideal values. Therefore, by using the TOPSIS method, the best combinations of experimental runs for machine sound level can be arranged as $1 - 2 - 3 - 4 - 6 - 7 - 9 - 5 - 8$. For machine vibration rate, the best arrangement by TOPSIS is $2 - 1 - 6 - 9 - 7 - 8 - 3 - 5 - 4$. Table 14 verified that the feed rate at 0.10 mm/rev (0.5139), depth of cut at 0.75 mm (0.5339), and spindle speed at 355 rev/min (0.8021) are the ideal values of parameters obtained by the TOPSIS approach for machine sound level. Similarly, optimum values for machine vibration rate as shown in Table 15 are spindle speed (level 1), feed rate (level 2), and depth of cut (level 2). These optimum values of parameters are for obtaining better machining performance during the turning of AISI 1525 steel. Figures 12 and 13 report on Taguchi analysis (main effect plot for relative closeness) for each of the response variables. The machine

Fig. 12 Main effect plot of relative closeness for machine sound level
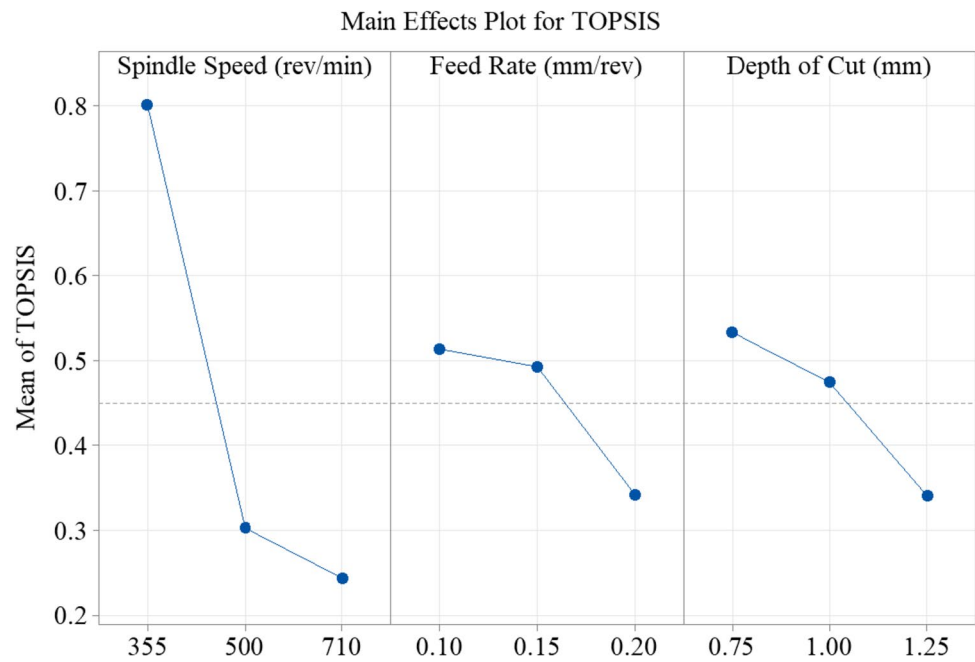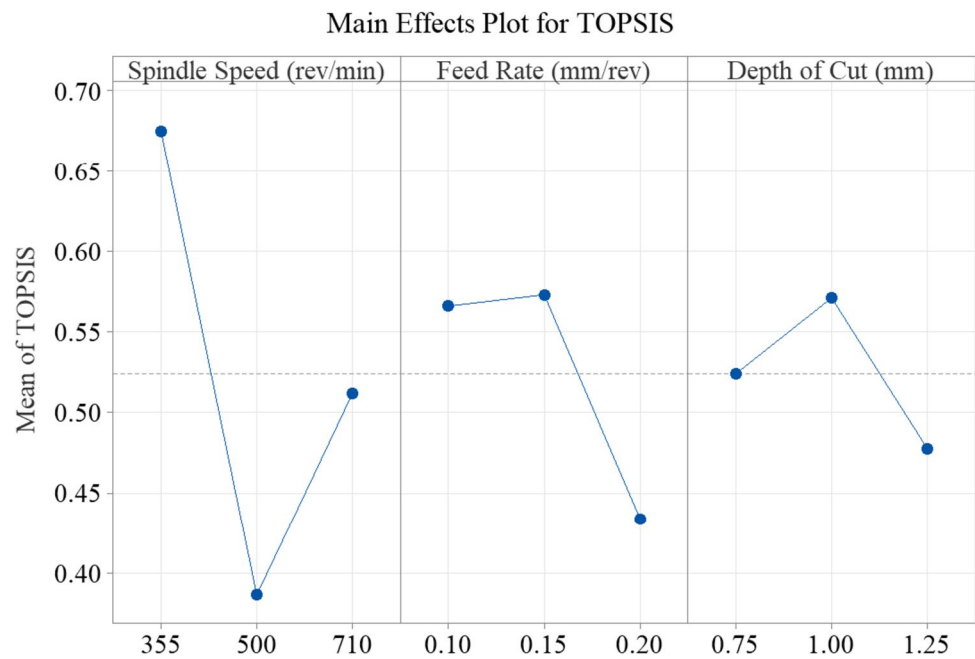

Fig. 13 Main effect plot of relative closeness for machine vibration rate

sound level is shown in Fig. 12, and the best result for the attribute was obtained by combining 355 rev/min (SS), 0.10 mm/rev (FR), and 0.75 mm (DOC). The optimal machine vibration rate is determined by a combination of 355 rev/min (SS), 0.15 mm/rev (FR), and 1.00 mm (DOC), as shown in Fig. 13. A study was carried out to ascertain the importance of three cutting parameters: feed rate, depth of cut, and spindle speed. Using Minitab software, an analysis of variance was conducted as part of this inquiry. The ANOVA analysis findings that were obtained to evaluate the influence of input parameters on

the machine sound level and vibration rate are shown in Table 16. It offers details on how these input elements' statistical significance affects the observed output variables. Spindle speed has the most effect of all the output factors, contributing 81.08% to machine sound level, as Table 16 illustrates. In AISI turning processes using tungsten carbide tools, spindle speed has a greater impact on machine sound level than feed rate (7.53%) and depth of cut (8.44%). Spindle speed, feed rate, depth of cut, and machine vibration rate all contributed differently: 55.20%, 16.26%, and 5.77%, respectively. According to

Table 16 Results of ANOVA on relative closeness for response variables

Parameter	Source	DOF	Seq SS	Adj SS	Adj MS	F-Value	Contribution%
MVR	SS	2	0.12549	0.12549	0.062744	2.42	55.20%
	FR	2	0.03696	0.03696	0.018482	0.71	16.26%
	DOC	2	0.01311	0.01311	0.006557	0.25	5.77%
	Error	2	0.05176	0.05176	0.025878		22.77%
	Total	8	0.22732				100.00%
MSL	SS	2	0.56353	0.56353	0.28177	27.51	81.08%
	FR	2	0.05235	0.05235	0.02618	2.56	7.53%
	DOC	2	0.05868	0.05868	0.02934	2.86	8.44%
	Error	2	0.02048	0.02048	0.01024		2.95%
	Total	8	0.69504				100.00%

the investigation, among all the input elements that go into MVR, the DOC showed the least amount of significance.

3.8 Mathematical Models

Equations ([11]) through ([26]) provided regression equations to determine the relationship between the independent and dependent variables. To recommend the optimal equation, the determination coefficient (R^2) was also computed for the dependent variables. Regression analysis was used in this study to generate mathematical models employing feed rate, depth of cut, and spindle speed as input parameters for turning AISI 1525 steel. Minitab software was used to analyze experimental data and develop an optimization model for machine vibration and machine sound level for different cooling and lubricating fluids.

Jatropha oil emulsion models

$$MSL = -64.2 + 0.4516SS + 486FR - 0.000321SS^2 - 707FR^2 - 0.4308(SS \times FR) \tag{11}$$

$$MSL = -17.0 + 0.4610SS - 33.5DOC - 0.000321SS^2 + 40.5DOC^2 - 0.0740(SS \times DOC) \tag{12}$$

$$MVR = -108.9 + 0.3253SS + 391FR - 0.000223SS^2 - 955FR^2 - 0.160(SS \times FR) \tag{13}$$

$$MVR = -87.5 + 0.3241SS + 5.6DOC - 0.000223SS^2 + 8.2DOC^2 - 0.0228(SS \times DOC) \tag{14}$$

Mineral oil emulsion models

$$MSL = 32.9 + 0.116SS + 156FR - 0.000044SS^2 - 193FR^2 - 0.024(SS \times FR) \tag{15}$$

$$MSL = 138 + 0.130SS - 177DOC - 0.000044SS^2 + 87.5DOC^2 - 0.0174(SS \times DOC) \tag{16}$$

$$MVR = 137 + 0.083SS - 307DOC - 0.000139SS^2 + 148DOC^2 + 0.073(SS \times DOC) \tag{17}$$

$$MVR = 184 - 562FR - 285DOC + 1624FR^2 + 148DOC^2 + 103(FR \times DOC) \tag{18}$$

Jatropha MQL models

$$MSL = -4.9 + 0.2889SS + 231FR - 0.000200SS^2 - 353FR^2 - 0.295(SS \times FR) \tag{19}$$

$$MSL = 33.1 + 0.2214SS - 24.8DOC - 0.000200SS^2 + 12.3DOC^2 + 0.0232(SS \times DOC) \tag{20}$$

$$MVR = -12.0 + 0.1274SS - 45.2DOC - 0.000123SS^2 + 25.7DOC^2 + 0.0084(SS \times DOC) \tag{21}$$

$$MVR = -17.9 + 439FR - 27.7DOC - 1221FR^2 + 25.7DOC^2 - 87(FR \times DOC) \tag{22}$$

Mineral MQL models

$$MSL = -25.2 + 0.631SS - 571FR - 0.000502SS^2 + 2840FR^2 - 0.445(SS \times FR) \tag{23}$$

$$MSL = -123.3 + 0.548SS + 149DOC - 0.000502SS^2 - 65.6DOC^2 + 0.0163(SS \times DOC) \tag{24}$$

$$MVR = -312 + 1.943SS - 2170FR - 0.001609SS^2 + 9979FR^2 - 1.247(SS \times FR) \tag{25}$$

$$MVR = -504 + 1.754SS + 164DOC - 0.001609SS^2 - 54DOC^2 + 0.001(SS \times DOC) \tag{26}$$

Here, Table 17 shows that the R^2 values of the second-order models were much closer to 1. Representing the best fit of the model, it shows how closely predicted values match the experimental data and is deemed statistically significant and satisfactory. It follows that the second-order model that was developed indicates a strong link between the predicted and experimental results. Based on this comparison analysis,

it can be safely concluded that the second-order model that was developed can predict the expected results before the experiment involving the turning of AISI 1525 steel

3.9 Evaluation of Contour and Surface Plots

Figure 14 presents a comprehensive analysis of the intricate association between MSL, the dependent variable, and the independent variables of FR and DOC. Notably, a distinct valley is discernible, indicating a specific range of FR (0.14–0.16 mm/rev) and DOC (0.95–1.05 mm), where the machine sound level reaches its minimum levels, measuring approximately 89 dB. Further examination of the contour lines within the plot reveals a noteworthy characteristic: their overall curvature. This curvature signifies that the rate of change in both FR and DOC varies non-linearly between the contour lines. Such behavior emphasizes the interactive nature of these cutting parameters, as their combined influence significantly affects machine sound levels. It is worth noting that the contour lines illustrate that their collective impact on machine sound level exceeds what could have been predicted by considering each factor in isolation. Figure 15 showcases a surface plot characterized by an irregular concave shape, effectively illustrating the non-linear relationship among the FR, DOC, and MSL. The sought-after optimal minimum value for MSL, approximately 89 dB, is achieved by configuring the FR to 0.15 mm/rev and the DOC to 1.00 mm. It is important to note that the plot reveals asymmetry, indicating that MSL does not respond equally to changes in the FR and DOC, irrespective of the direction of adjustment. This asymmetry suggests that modifications in either parameter will not exert a comparable influence on MSL. Figure 16 presents a comprehensive analysis of the intricate association between MVR, the dependent variable, and the independent variables of FR and DOC. Notably, a

Table 17 Corresponding S and R^2 values

Eq. No	S	R^2
11	1.353	99.13%
12	2.645	96.66%
13	3.355	96.18%
14	2.371	98.09%
15	7.499	84.40%
16	7.444	84.63%
17	11.486	56.60%
18	11.982	52.77%
19	3.079	90.99%
20	2.002	96.19%
21	3.502	68.25%
22	3.714	64.29%
23	9.021	76.01%
24	6.818	86.30%
25	15.851	90.35%
26	24.068	77.76%

Fig. 14 Contour plot of FR, DOC, and MSL for jatropha oil emulsion
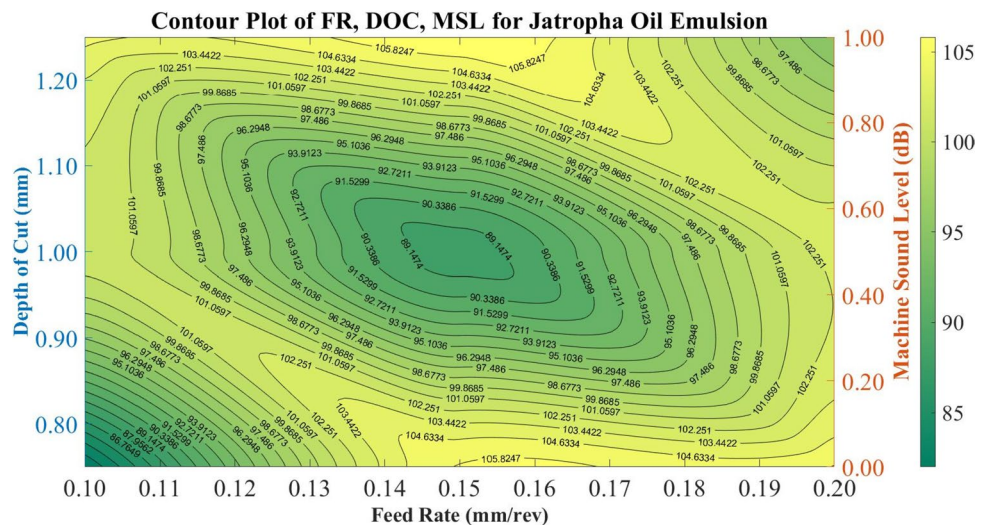
Fig. 15 Surface plot of FR, DOC, and MSL for jatropha oil emulsion
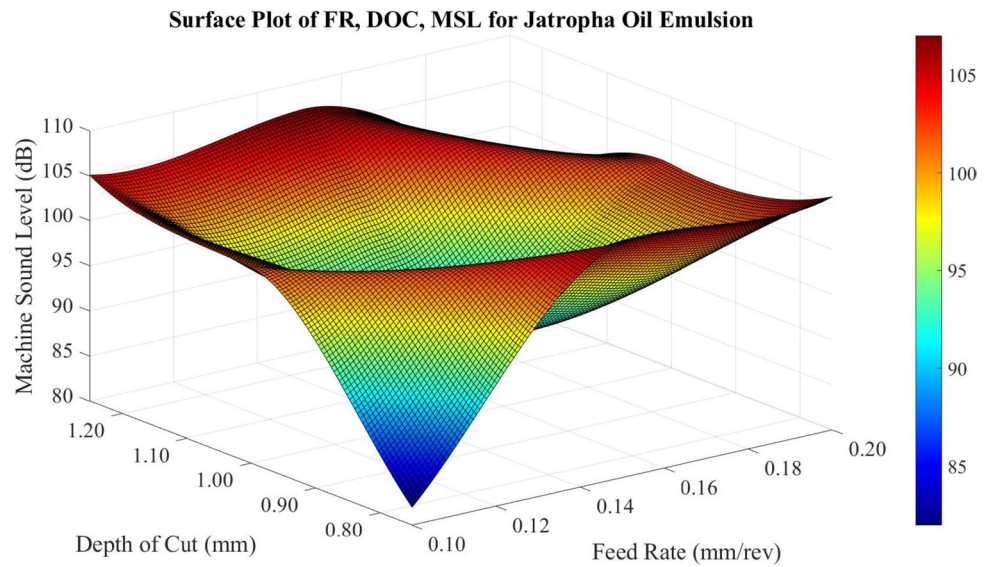
distinct valley is discernible, indicating a specific range of FR (0.14–0.16 mm/rev) and DOC (0.95–1.05 mm) where the machine vibration reaches its minimum levels, measuring approximately 7 m/s^2. Further examination of the contour lines within the plot reveals a noteworthy characteristic: their overall curvature. This curvature signifies that the rate of change in both FR and DOC varies non-linearly between the contour lines. Such behavior emphasizes the interactive nature of these cutting parameters, as their combined influence significantly affects machine vibration. It is worth noting that the contour lines illustrate that their collective impact on machine vibration exceeds what could have been predicted by considering each factor in isolation.

Figure 17 showcases a surface plot characterized by an irregular concave shape, effectively illustrating the non-linear relationship among the FR, DOC, and MVR. The

sought-after optimal minimum value for MVR, approximately 7 m/s^2, is achieved by configuring the FR to 0.15 mm/rev and the DOC to 1.00 mm. It is important to note that the plot reveals asymmetry, indicating that MVR does not respond equally to changes in the FR and DOC, irrespective of the direction of adjustment. This asymmetry suggests that modifications in either parameter will not exert a comparable influence on MVR. Figure 18 presents a comprehensive examination of the relationship between machine sound level, the response variable, and the independent variables of SS and DOC. Notably, a distinct peak or valley is not observed in this plot; however, there are clear trends that can be discerned. As SS increases, the machine sound level gradually increases until it reaches a plateau. At low SS values, an increase in DOC is associated with a slight increase in machine sound levels, whereas at higher

Fig. 16 Contour plot of FR, DOC, and MVR for jatropha oil emulsion
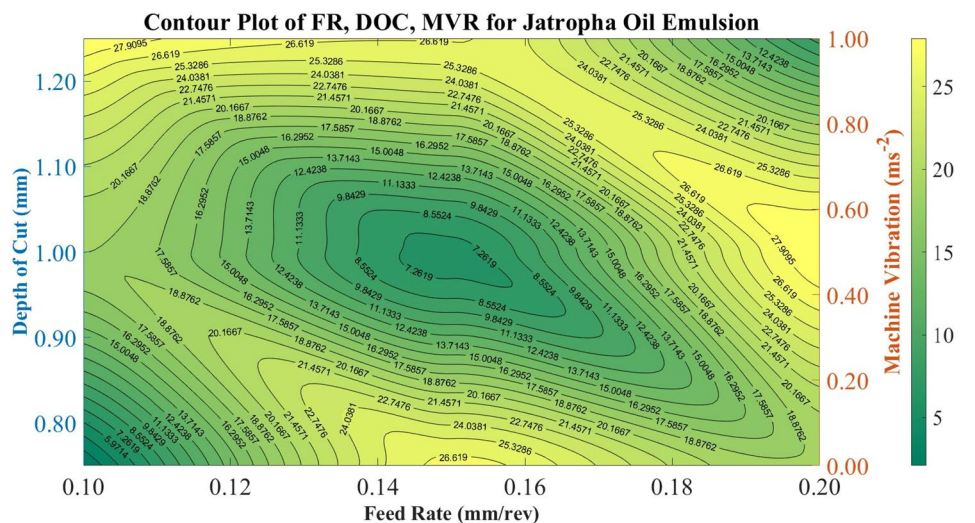
Fig. 17 Surface plot of FR, DOC, and MVR for jatropha oil emulsion
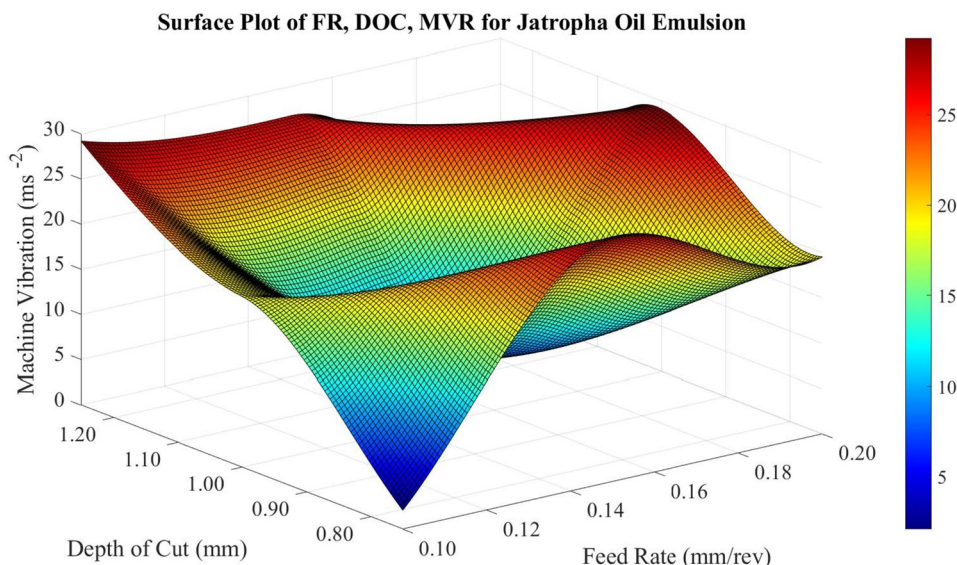
SS values (> 550 rev/min), changes in both the DOC and SS do not affect machine sound levels significantly.

Analyzing the contour lines within the plot reveals intriguing characteristics. At lower machine sound levels, the contour lines exhibit a generally curved nature, indicating non-constant changes in the cutting parameters. Conversely, at higher machine sound levels, the contour lines demonstrate a more linear nature, suggesting more consistent changes in the cutting parameters. The contour lines indicate varying degrees of interaction between the cutting parameters based on the machine sound level. At lower machine sound levels, there is a higher level of interaction between the cutting parameters, whereas at higher machine sound levels, the interactions are comparatively less. Figure 19 depicts a regular surface plot, which effectively conveys the existence of a linear correlation between

SS, DOC, and machine sound levels. Remarkably, the investigation reveals that the most favorable outcome in terms of minimal machine sound levels, approximately 84 dB, can be attained by configuring the SS to 350 rev/min and the DOC to 0.75 mm. The plateau at SS values higher than 550 rev/min indicates that variation in the cutting parameters, SS and DOC, in this region has no significant influence on the machine sound levels. Figure 20 presents a comprehensive examination of the relationship between machine vibration, the response variable, and the independent variables of SS and DOC. A distinct peak or valley is not observed in this plot; however, the contour lines within the plot display a parallel and linear orientation throughout. The contour plot shows that as SS increases, the machine vibration gradually increases until it reaches a plateau (SS > 550 rev/min), and in this region, changes in SS and DOC do not affect machine

Fig. 18 Contour plot of SS, DOC, and MSL for jatropha oil emulsion
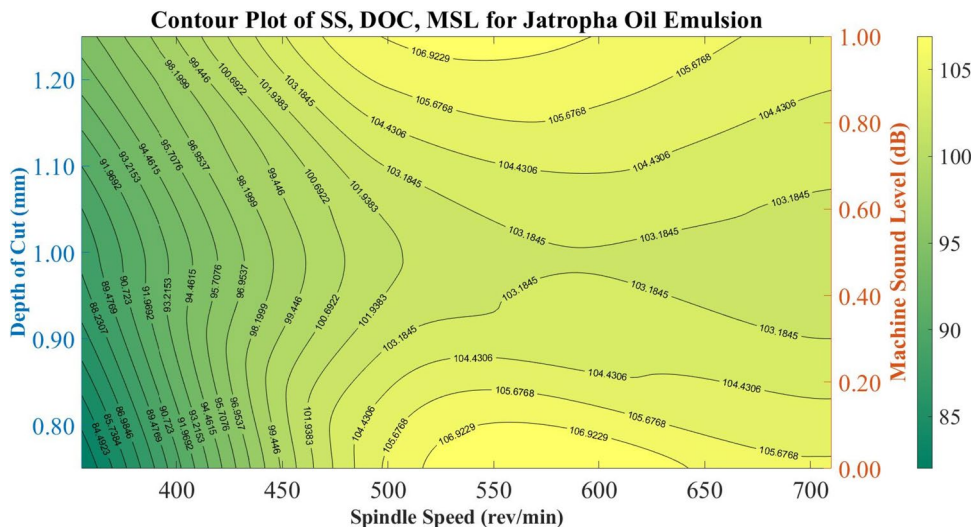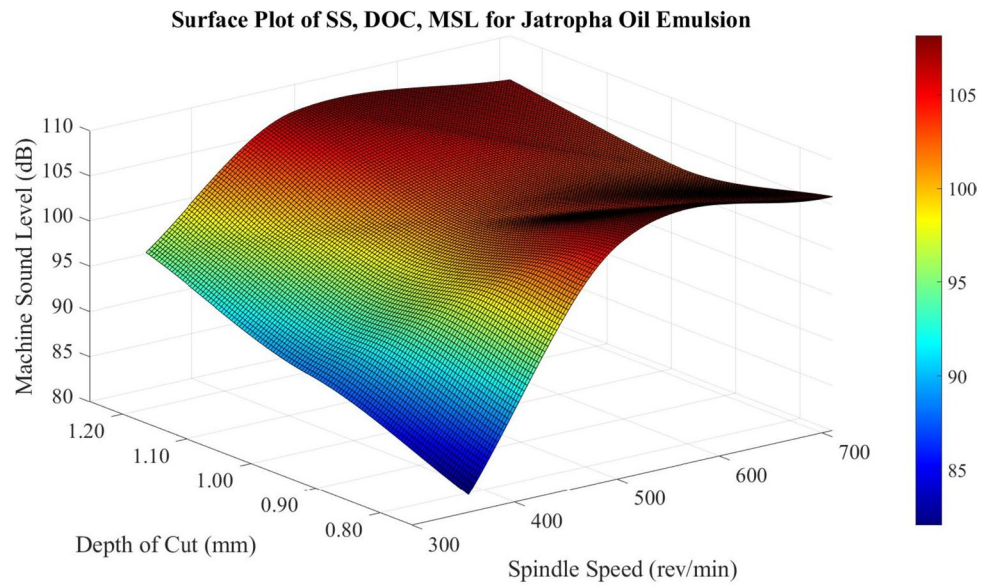
vibrations significantly. The plot indicates that changes in SS and DOC occur at a constant rate and act independently to influence machine vibrations, with minimal interaction between the two variables. The parallel and linear nature of the contour lines suggests that adjustments in SS and DOC can be made separately and without significant consideration of their combined effect on machine vibrations. The surface plot depicted in Fig. 21 exhibits a regular shape, indicating a linear relationship between the SS, DOC, and MVR. The plot highlights a minimum MVR value of approximately 4.5 m/s^2, achieved when the SS is set at 350 rev/min and the DOC is set at 0.75 mm. Observing the plot, it becomes apparent that the MVR is only slightly sensitive to changes in the DOC, but highly sensitive to changes in the SS in the region SS < 550 rev/min, as indicated by the relatively steep slope. This sensitivity implies that slight adjustments in the

SS would result in significant alterations in MVR in this region. Figure 22 presents a comprehensive examination of the relationship between machine sound level, the response variable, and the independent variables of SS and FR. At low SS values (SS < 450 rev/min), the contour lines within the plot display a parallel and linear orientation and display an overall curvature at higher SS values. The contour plot shows that as SS increases, the machine sound level gradually increases until it reaches a plateau (SS > 550 rev/min). The plot reveals a significant linear relationship between the SS, FR, and MSL, where the minimum MSL is obtained by minimizing the independent variables SS and FR. The MSL reaches a peak in the region SS > 550 rev/min, where changes in the SS and FR only affect the MSL slightly. The parallel and linear nature of the contour lines in the region SS < 550 rev/min suggests that adjustments in SS and FR can

Fig. 20 Contour plot of SS, DOC, and MVR for jatropha oil emulsion
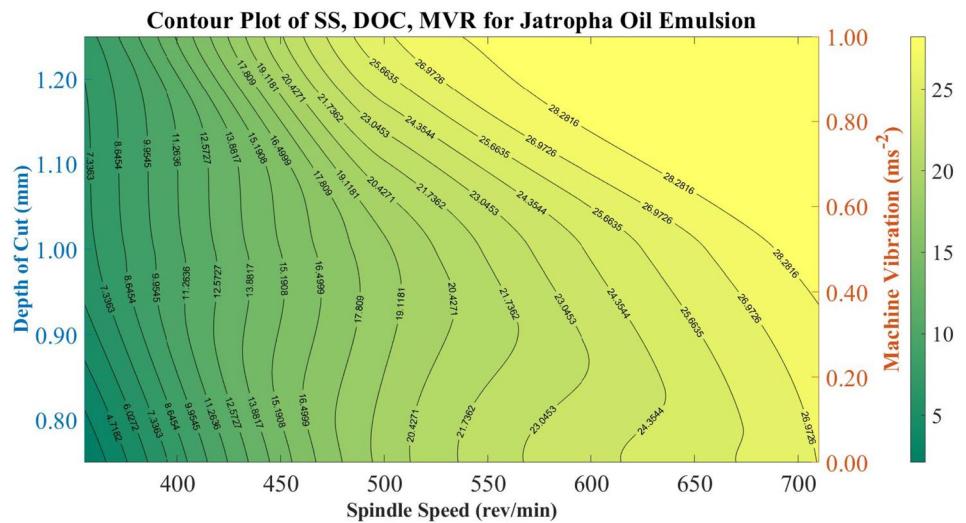
Fig. 21 Surface plot of SS, DOC, and MVR for jatropha oil emulsion
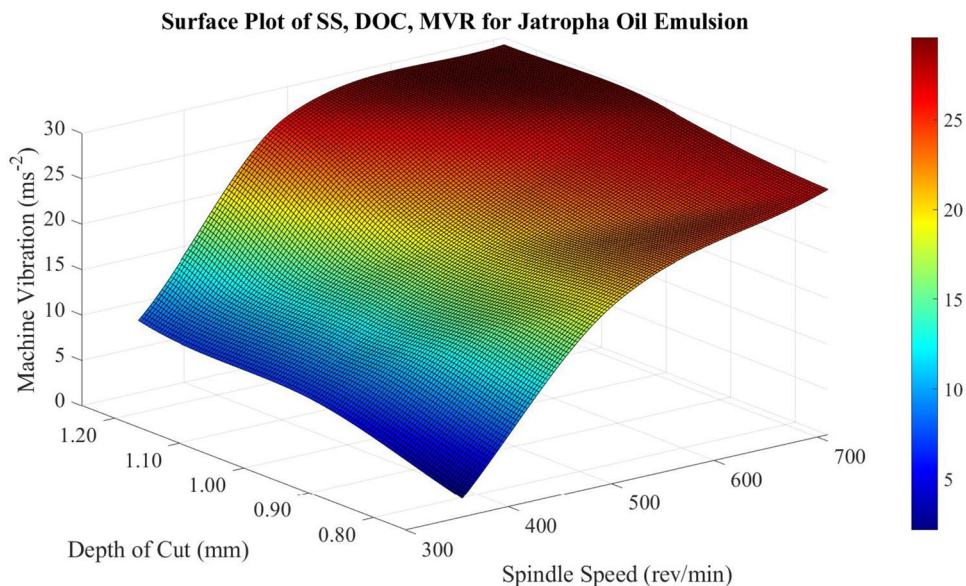
Fig. 22 Contour plot of SS, FR, and MSL for jatropha oil emulsion
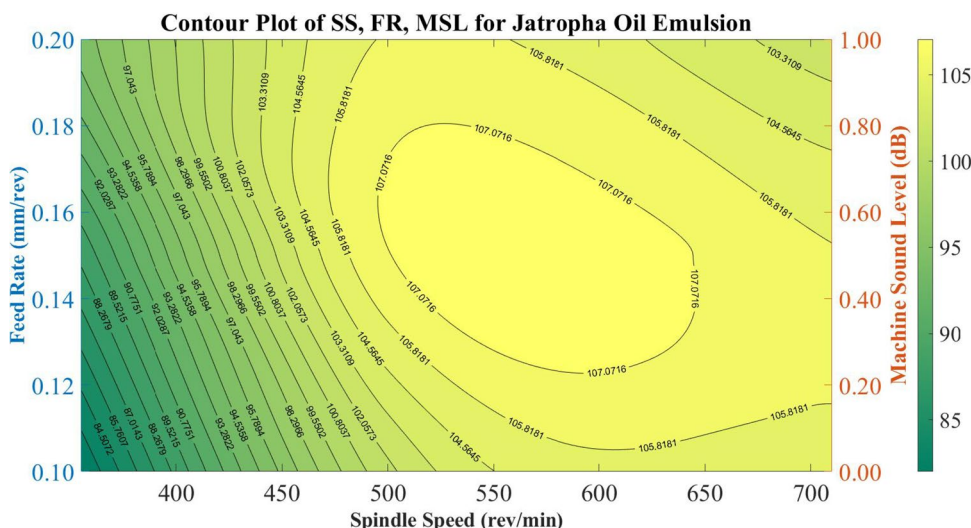
be made separately and without significant consideration of their combined effect on machine sound levels. The surface plot depicted in Fig. 23 exhibits a regular shape, indicating a linear relationship between the SS, FR, and MSL. The plot highlights a minimum MSL value of approximately 84 dB, achieved when the SS is set at 350 rev/min and the FR is set at 0.1 mm/rev. Observing the plot, it becomes apparent that the MSL is slightly sensitive to changes in the FR, but highly sensitive to changes in the SS in the region SS < 450 rev/min, as indicated by the relatively steep slope. This sensitivity implies that relatively small adjustments in the SS would result in significant alterations in MSL in this region.

Figure 24 presents a comprehensive examination of the relationship between machine vibration, the response variable, and the independent variables of SS and FR. The contour plot has an overall curvature showing strong interaction between the cutting parameters, SS and FR, to control the response variable, MVR. A distinct valley or peak is not present and the influence of the cutting parameters on the machine vibration reduces as the spindle speed increases. The minimum vibration, approximately 4.5 m/s^2, is obtained by minimizing the SS and the FR values. The surface plot depicted in Fig. 25 exhibits a slightly irregular shape, indicating a non-linear relationship between the SS, FR, and MVR. The plot highlights a minimum MVR value of approximately 4.5 m/s^2, achieved when the SS is set at 350 rev/min and the FR is set at 0.1 mm/rev. Observing the plot, the relatively steep slope at low SS values, SS < 500 rev/min, shows that the MVR is highly sensitive to changes in the SS value in this region. This sensitivity implies that relatively small adjustments in the SS would result in significant alterations in MVR in this region. Figure 26 presents a

Fig. 23 Surface plot of SS, FR, and MSL for jatropha oil emulsion
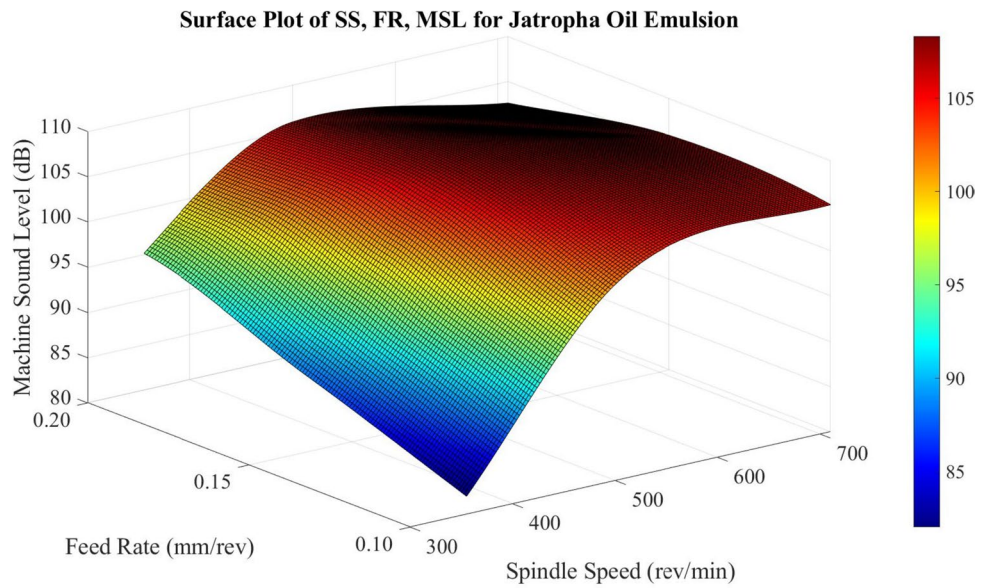
Fig. 24 Contour plot of SS, FR, and MVR for jatropha oil emulsion
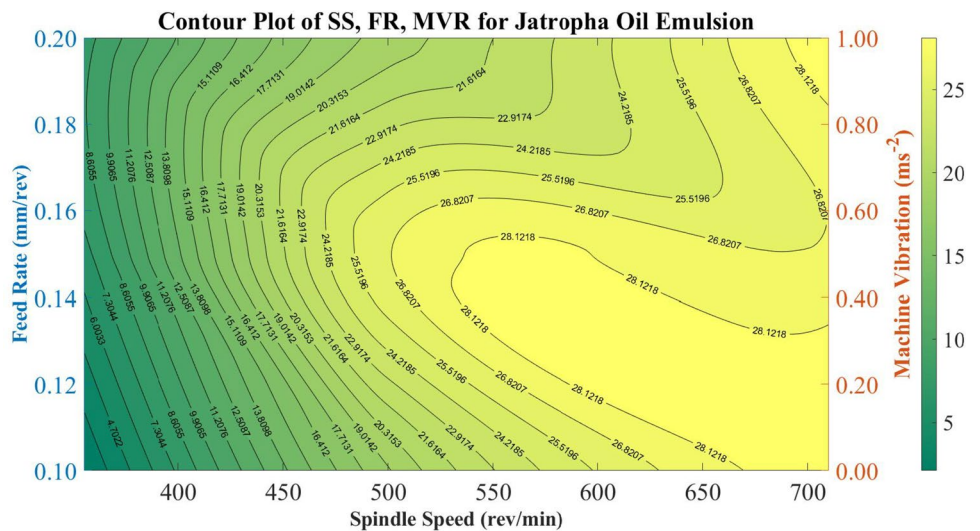
comprehensive analysis of the intricate association between MSL, the dependent variable, and the independent variables of FR and DOC. Notably, a distinct valley is discernible, indicating a specific range of FR (0.15–0.165 mm/rev) and DOC (0.95–1.00 mm), where the machine sound level reaches its minimum levels, measuring approximately 83 dB. Further examination of the contour lines within the plot reveals a noteworthy characteristic: their overall curvature. This curvature signifies that the rate of change in both FR and DOC varies non-linearly between the contour lines. Such behavior emphasizes the interactive nature of these cutting parameters, as their combined influence significantly affects machine sound levels. It is worth noting that the contour lines illustrate that their collective impact on machine sound level exceeds what could have been predicted by considering each factor in isolation. Figure 27 showcases

a surface plot characterized by an irregular concave shape, effectively illustrating the non-linear relationship among the FR, DOC, and MSL. The sought-after optimal minimum value for MSL, approximately 83 dB, is achieved by configuring the FR to 0.15 mm/rev and the DOC to 1.00 mm. It is important to note that the plot reveals asymmetry, indicating that MSL does not respond equally to changes in the FR and DOC, irrespective of the direction of adjustment. This asymmetry suggests that modifications in either parameter will not exert a comparable influence on MSL. Figure 28 analyses the relationship between the independent variables, FR and DOC, and their influence on the response variable, MVR. A distinct peak can be observed, representing the combinations of FR and DOC that yield the highest MVR. The peak, with an MVR of approximately 13.4 m/s^2, occurs when the FR ranges from 0.14 to 0.16 mm/rev and the DOC

Fig. 25 Surface plot of SS, FR, and MVR for jatropha oil emulsion
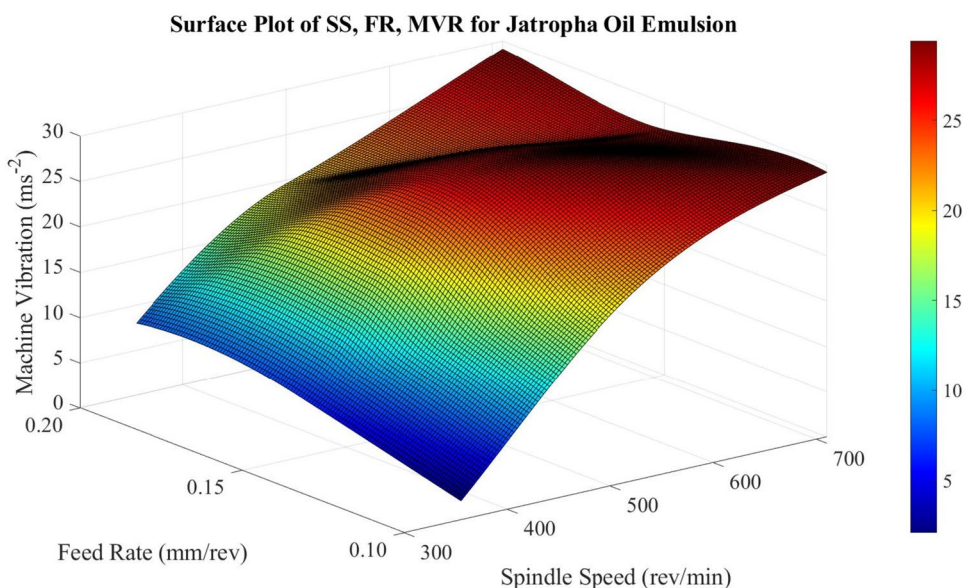
Fig. 26 Contour plot of FR, DOC, and MSL for jatropha oil MQL
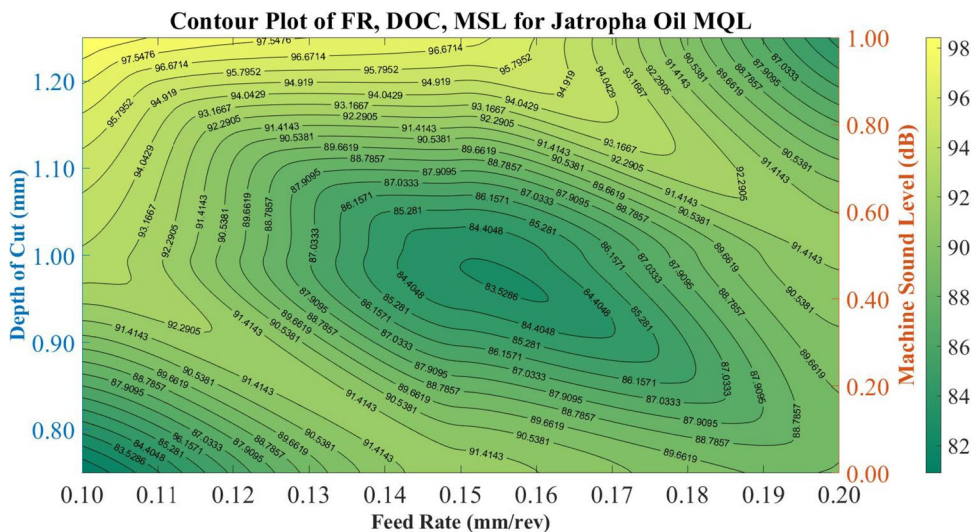
ranges from 1.2 to 1.25 mm. Conversely, a valley in the plot with an MVR of approximately 2.3 m/s^2 is obtained when the FR ranges from 0.14 to 0.2 mm/rev, and the DOC ranges from 0.75 to 1.00 mm. The contour lines within the plot display curved shapes and are more concentrically spaced than parallel. This suggests that the FR and DOC interact with each other, resulting in a combined effect on the MVR that exceeds the impact of either factor acting in isolation. The non-linear and concentric nature of the contour lines indicates that adjustments to both FR and DOC are necessary to effectively control and optimize MVR. The surface plot depicted in Fig. 29 exhibits an irregular shape, indicating a non-linear relationship between the FR, DOC, and MVR. To accurately capture this complex relationship, advanced modeling techniques such as polynomial regression, spline

regression, or machine learning algorithms can be employed. The desired optimal minimum value for MVR is approximately 2.3 m/s^2, achieved when the FR is set at 0.2 mm/ rev and the DOC is set at 0.75 mm. Notably, the plot demonstrates asymmetry, suggesting that MVR is not equally responsive to changes in the FR and DOC, regardless of the direction of adjustment.

This asymmetry implies that adjustments in either parameter will not have a comparable impact on MVR. Figure 30 presents a comprehensive examination of the relationship between machine sound level, the response variable, and the independent variables of SS and DOC. A peak with an MSL of approximately 98.5 dB can be observed when the SS ranges from 600 to 700 rev/min and the DOC ranges from 1.2 to 1.25 mm. The contour lines within the plot

Fig. 27 Surface plot of FR, DOC, and MSL for jatropha oil MQL
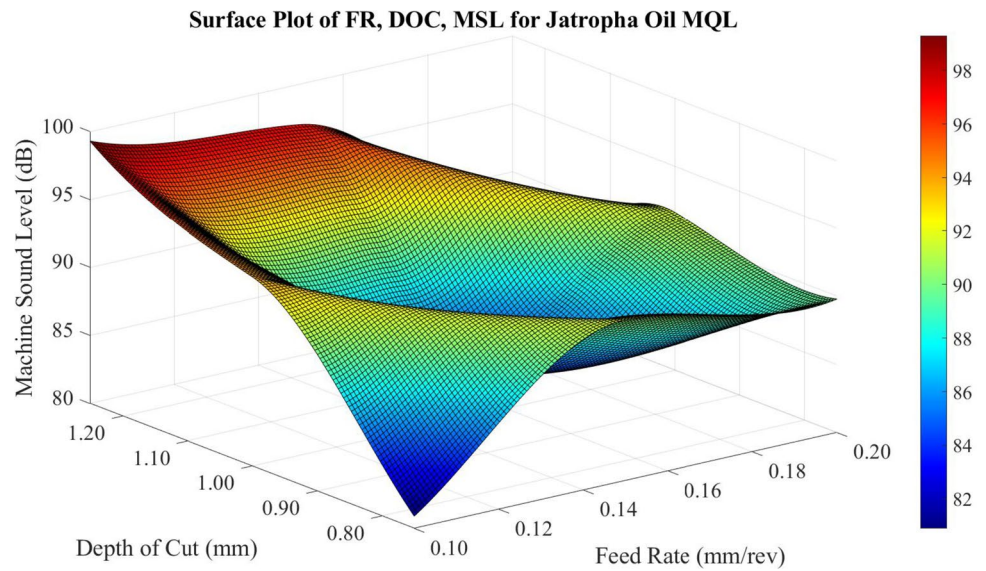
Fig. 28 Contour plot of FR, DOC, and MVR for jatropha oil MQL
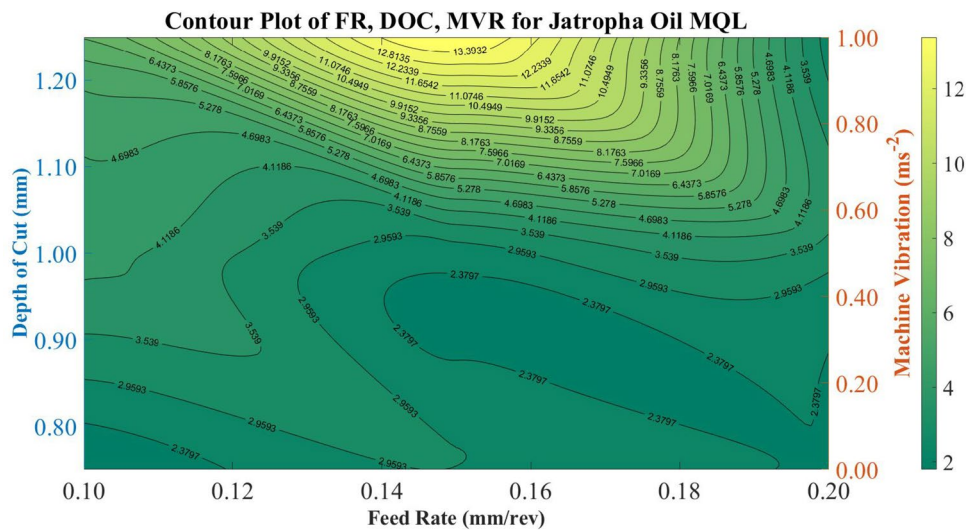
display an approximately parallel and linear orientation in the region SS < 450 rev/min. The contour plot shows that as SS increases, the machine sound level gradually increases until it reaches a plateau (SS > 500 rev/min). In this region, changes in SS and DOC do not affect machine sound levels significantly. In the region SS < 450 rev/min, the plot indicates that changes in SS and DOC occur at a constant rate and act independently to influence machine sound levels, with minimal interaction between the two variables. The parallel and linear nature of the contour lines in this region suggests that adjustments in SS and DOC can be made separately and without significant consideration of their combined effect on machine sound levels. The surface plot depicted in Fig. 31 exhibits a regular shape, indicating a significant linear relationship between the SS, DOC, and MSL. The plot highlights a minimum MSL value of approximately

98.5 dB, achieved when the SS is set at 700 rev/min and the DOC is set at 1.25 mm. Observing the plot, it becomes apparent that the MSL is only slightly sensitive to changes in the DOC, but highly sensitive to changes in the SS in the region SS < 450 rev/min, as indicated by the relatively steep slope. This sensitivity implies that slight adjustments in the SS would significantly alter MSL in this region. Figure 32 showcases the relationship between the independent variables, SS and DOC, and their impact on the response variable, MVR. Notably, the plot reveals a distinct peak representing a high MVR and a corresponding valley representing a low MVR. The peak, characterized by an MVR of approximately 13.4 m/s^2, is achieved when the SS ranges from 500 to 550 rev/min, and the DOC varies from 1.2 to 1.25 mm. Conversely, the valley, reflecting an MVR of about 2.3 m/s^2, corresponds to an SS range of 350 to 500 rev/min,

Fig. 29 Surface plot of FR, DOC, and MVR for jatropha oil MQL
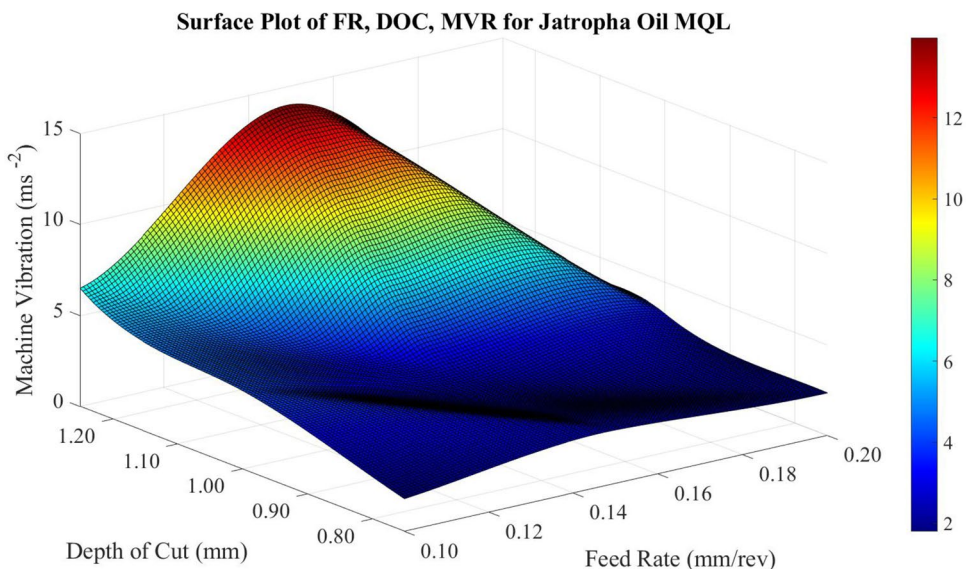
Fig. 30 Contour plot of SS, DOC, and MSL for jatropha oil MQL
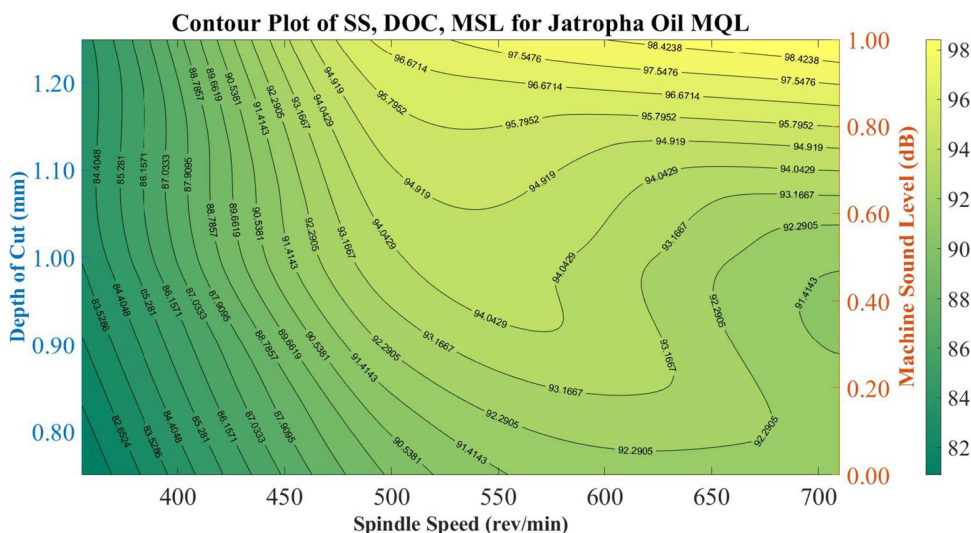
and a DOC ranging from 0.75 to 0.90 mm. Examining the contour lines within the plot, they display curved shapes and are more concentrically spaced rather than parallel. This suggests that the interaction between SS and DOC has a significant influence on altering the MVR, surpassing the individual effects of each factor. The non-linear and concentric nature of the contour lines highlights the importance of considering the combined impact of both variables when optimizing MVR. Figure 33 showcases a surface plot with an irregular convex shape, representing the relationship between the DOC, SS, and MVR. This shape indicates a non-linear association among these variables. Specifically, it reveals that as the DOC increases, the MVR experiences an increase. The plot indicates a minimum MVR of 2.3 m/s^2, which corresponds to an optimal DOC of 0.75 mm and an SS of 350 rev/min. The irregular convex shape of the plot

emphasizes the non-linear nature of the relationship between the DOC, SS, and MVR. It suggests that careful optimization of these parameters is crucial to achieving the desired MVR, as the rate of change in MVR varies across different regions of the plot. Figure 34 presents a comprehensive examination of the relationship between machine sound level, the response variable, and the independent variables of SS and FR. The contour plot has an overall curvature showing strong interaction between the cutting parameters, SS and FR, to control the response variable, MSL. A peak with a maximum MSL of approximately 98.5 dB can be observed when the SS ranges from 550 to 700 rev/min, and the FR ranges from 0.1 to 0.14 mm/rev. The minimum sound level, approximately 82 dB, is obtained by minimizing the SS and the FR values. The surface plot depicted in Fig. 35 exhibits a slightly irregular shape, indicating a non-linear relationship

Fig. 31 Surface plot of SS, DOC, and MSL for jatropha oil MQL
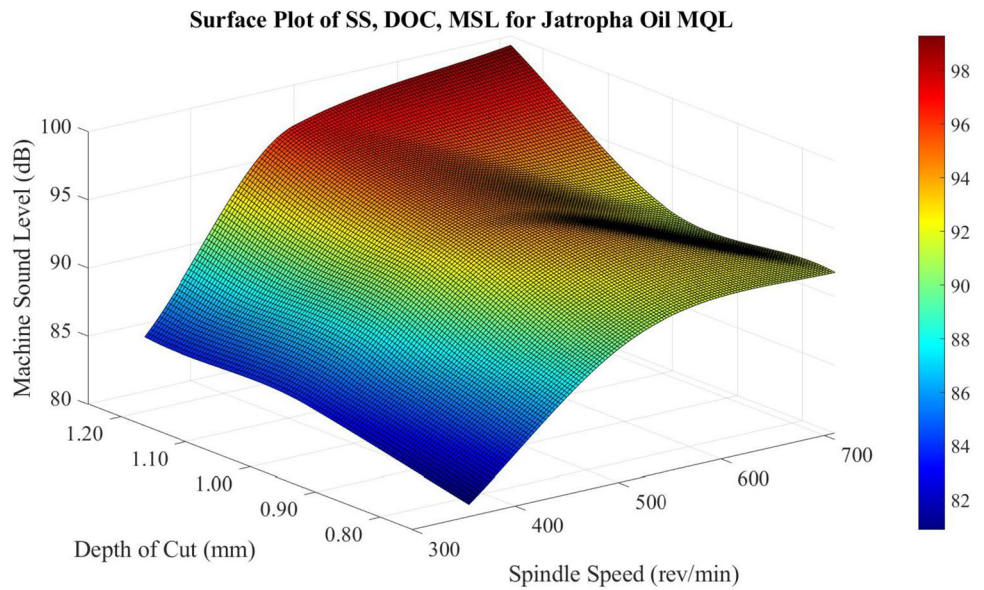
Fig. 32 Contour plot of SS, DOC, and MVR for jatropha oil MQL
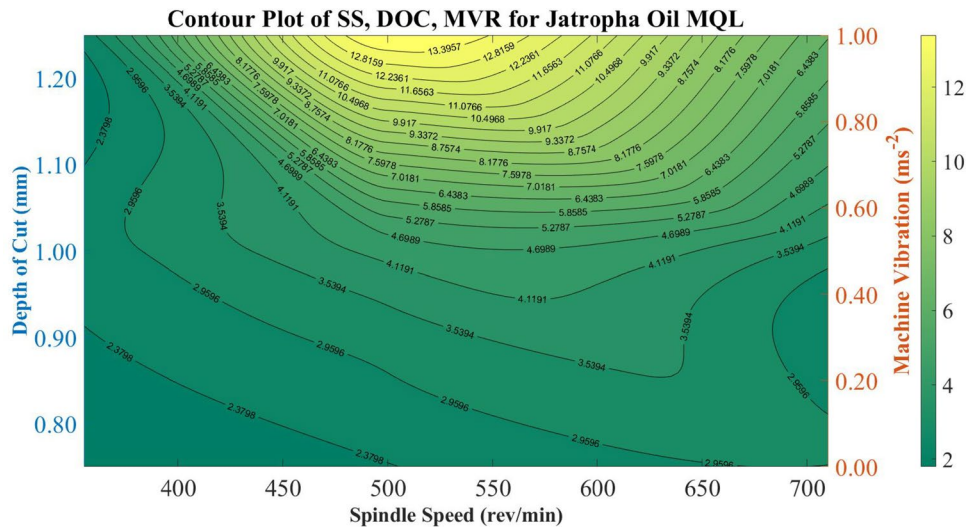
between the SS, FR, and MSL. The plot highlights a minimum MSL value of approximately 82 dB, achieved when the SS is set at 350 rev/min and the FR is set at 0.1 mm/rev.

Figure 36 presents a comprehensive analysis of the intricate association between MSL, the dependent variable, and the independent variables of FR and DOC. Notably, a distinct valley is discernible, indicating a specific range of FR (0.1–0.16 mm/rev) and DOC (0.95–1.05 mm), where the machine sound level reaches its minimum levels, measuring approximately 86 dB. Further examination of the contour lines within the plot reveals a noteworthy characteristic: their overall curvature. This curvature signifies that the rate of change in both FR and DOC varies non-linearly between the contour lines. Such behavior emphasizes the interactive nature of these cutting parameters, as their combined influence significantly affects machine sound levels. It is worth noting that the contour lines illustrate that their collective impact on machine sound level exceeds what could have been predicted by considering each factor in isolation. Figure 37 showcases a surface plot characterized by an irregular concave shape, effectively illustrating the non-linear relationship among the FR, DOC, and MSL. The sought-after optimal minimum value for MSL, approximately 86 dB, is achieved by configuring the FR to 0.14 mm/rev and the DOC to 1.00 mm. It is important to note that the plot reveals asymmetry, indicating that MSL does not respond equally to changes in the FR and DOC, irrespective of the direction of adjustment. This asymmetry suggests that modifications in either parameter will not exert a comparable influence on MSL, Fig. 38 showcases the relationship between the

Fig. 33 Surface plot of SS, DOC, and MVR for jatropha oil MQL
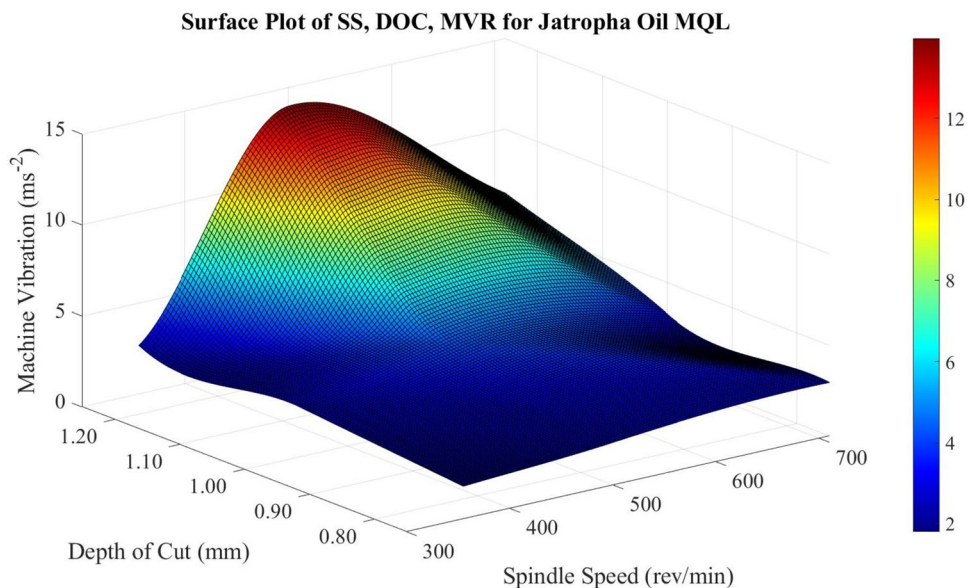
Fig. 34 Contour plot of SS, FR, and MSL for jatropha oil MQL
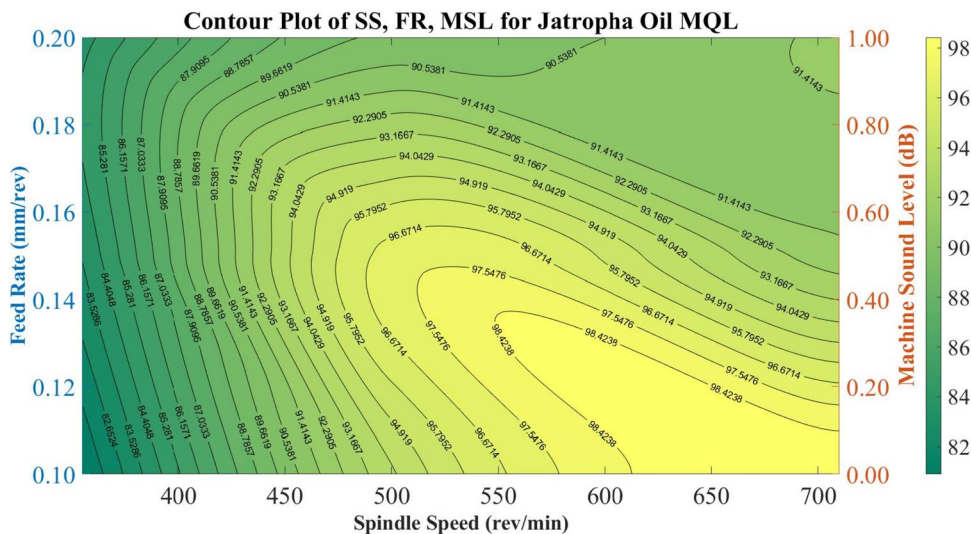
independent variables, FR and DOC, and their impact on the response variable, MVR. Notably, the plot reveals a distinct peak representing a high MVR and a corresponding valley representing a low MVR. The peak, characterized by an MVR of approximately 41.5 m/s^2, is achieved when the FR ranges from 0.14 to 0.17 mm/rev, and the DOC varies from 1.2 to 1.25 mm. Conversely, the valley, reflecting an MVR of about 7.9 m/s^2, corresponds to an FR range of 0.13 to 0.16 mm/rev, and a DOC ranging from 0.90 to 1.00 mm. Examining the contour lines within the plot, they display curved shapes and are more concentrically spaced rather than parallel. This suggests that the interaction between FR and DOC has a significant influence on altering the MVR, surpassing the individual effects of each factor. The non-linear and concentric nature of the contour lines highlights the importance of considering the combined impact of both variables when optimizing MVR. Figure 39 showcases a surface plot with an irregular convex shape, representing the relationship between the FR, DOC, and MVR. This shape indicates a non-linear association among these variables. The plot indicates a minimum MVR of 7.9 m/s^2, which corresponds to an optimal FR of 0.15 mm/rev and a DOC of 0.95 mm. The irregular convex shape of the plot emphasizes the non-linear nature of the relationship between the FR, DOC, and MVR. It suggests that careful optimization of these parameters is crucial to achieving the desired MVR, as the rate of change in MVR varies across different regions of the plot. Figure 40 presents a comprehensive analysis of the intricate association between MSL, the dependent variable, and the independent variables of SS and DOC. Notably, a

Fig. 35 Surface plot of SS, FR, and MSL for jatropha oil MQL

Surface Plot of SS, FR, MSL for Jatropha Oil MQL

Fig. 36 Contour plot of FR, DOC, and MSL for mineral oil emulsion
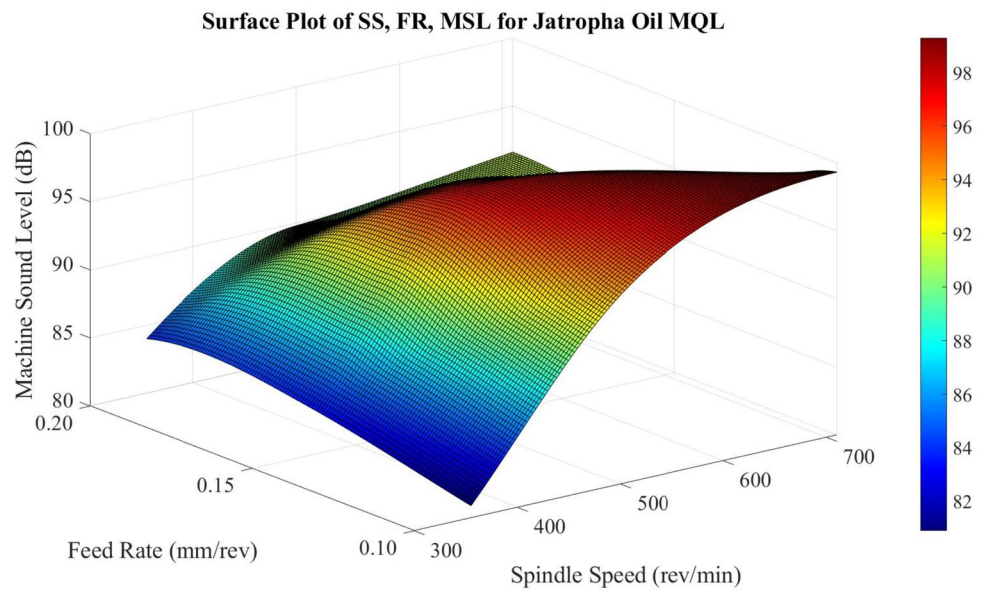
Contour Plot of FR, DOC, MSL for Mineral Oil Emulsion
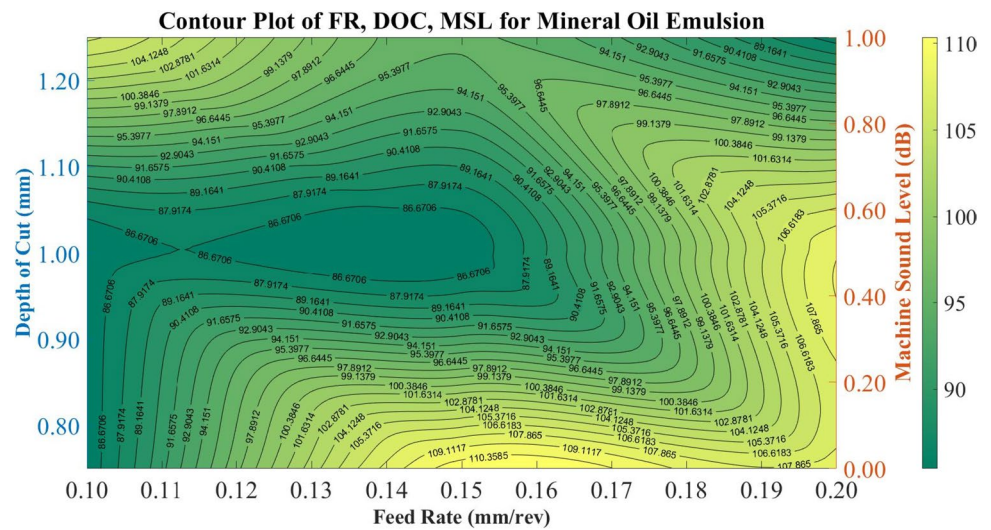
distinct valley is discernible, indicating a specific range of SS (350–500 rev/min) and DOC (1.0–1.20 mm) where the machine sound level reaches its minimum levels, measuring approximately 85 dB. Further examination of the contour lines within the plot reveals a noteworthy characteristic: their overall curvature. This curvature signifies that the rate of change in both SS and DOC varies non-linearly between the contour lines. Such behavior emphasizes the interactive nature of these cutting parameters, as their combined influence significantly affects machine sound levels. It is worth noting that the contour lines illustrate that their collective impact on machine sound level exceeds what could have been predicted by considering each factor in isolation. Figure 41 showcases a surface plot characterized by an irregular shape, effectively illustrating the non-linear relationship among the SS, DOC, and MSL. The sought-after optimal minimum value for MSL, approximately 85 dB, is

achieved by configuring the SS to 400 rev/min and the DOC to 1.10 mm.

It is important to note that the plot reveals asymmetry, indicating that MSL does not respond equally to changes in the SS and DOC, irrespective of the direction of adjustment. This asymmetry suggests that modifications in either parameter will not exert a comparable influence on MSL. Figure 42 offers a detailed examination of the relationship between machine vibration, the response variable, and the independent variables of SS and DOC. Notably, a distinct peak is observed, indicating the combination of SS ranging from 450–550 rev/min and DOC ranging from 1.2–1.25 mm, where machine vibrations reach their highest levels. The contour plot also reveals a distinct valley, indicating the combination of SS ranging from 350–400 rev/min and DOC ranging from 0.95–1.05 mm, where machine vibrations reach their lowest levels.

Fig. 37 Contour plot of FR, DOC, and MSL for mineral oil emulsion
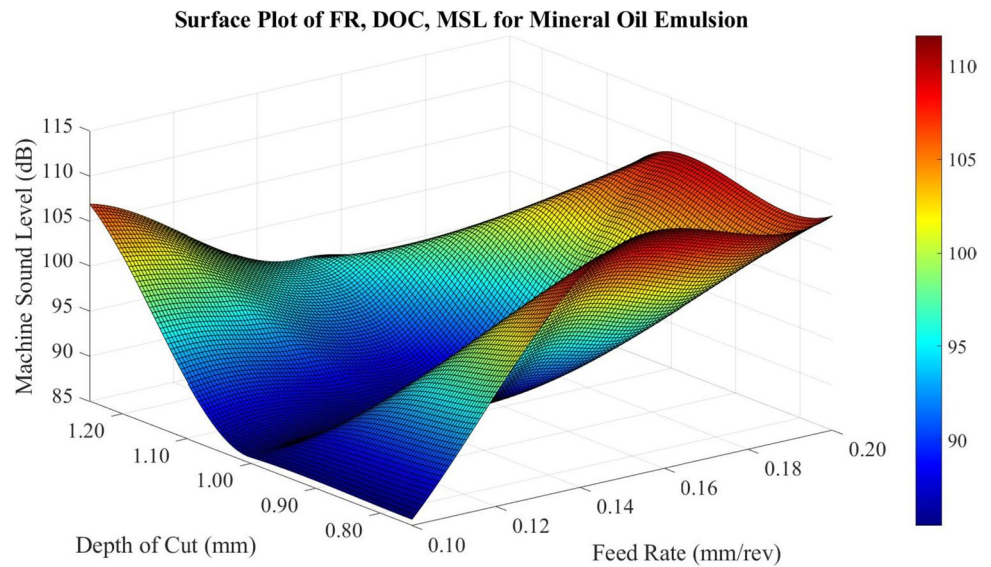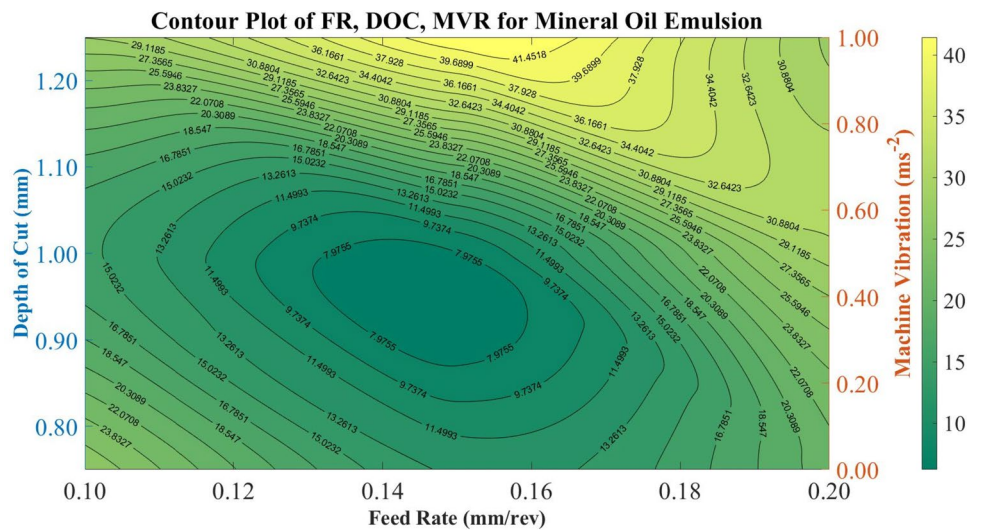

Fig. 38 Contour plot of FR, DOC, and MVR for mineral oil emulsion

Analyzing the contour lines within the plot reveals an interesting characteristic: their generally curved nature. This curvature signifies that the change in SS and DOC occurs at a non-constant rate between the contour lines. Such behavior highlights the interaction between these cutting parameters, as they collectively influence machine vibrations. The contour lines demonstrate that their combined effect alters machine vibrations to a greater extent than either factor acting alone would have predicted. Figure 43 illustrates an irregular surface plot, indicating a non-linear relationship between the SS, DOC, and MVR.

To accurately capture and understand this intricate relationship, sophisticated modeling techniques such as polynomial regression, spline regression, or machine learning algorithms can be employed. The optimal minimum value for machine vibration, approximately 9.5 m/s^2, is achieved by setting the SS to 350 rev/min and the DOC to 1.0 mm. It is important to note that the plot demonstrates asymmetry, suggesting that machine vibration does not equally respond to changes in the SS and DOC, regardless of the direction of adjustment. This indicates that modifications in either parameter cannot have an equivalent impact on vibration.

Fig. 39 Surface plot of FR, DOC, and MVR for mineral oil emulsion
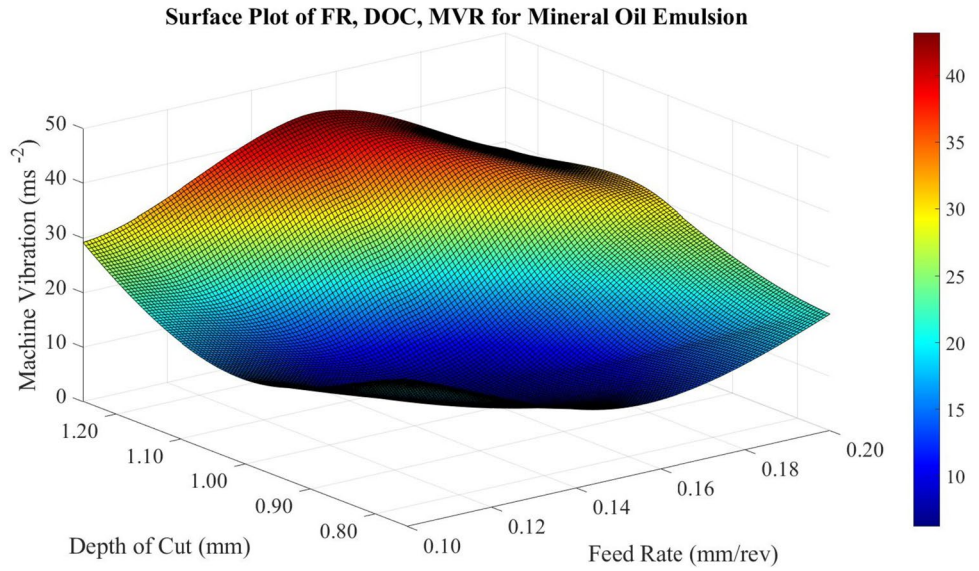
Fig. 40 Contour plot of SS, DOC, and MSL for mineral oil emulsion
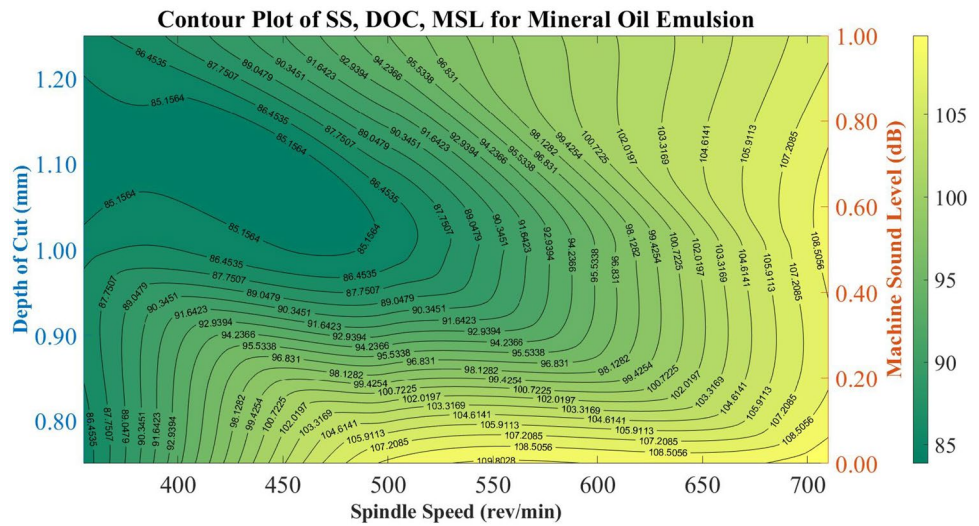
4 Conclusion

The purpose of this research was to demonstrate the efficacy of jatropha oil, both in its raw and emulsified forms, when turning AISI 1525 steel using a tungsten carbide tool. The experimental design used the Taguchi L9 orthogonal array. The following conclusions were made in light of the data.

- The jatropha emulsion and neat oils reduced machine vibration rate drastically more than their mineral oil equivalent. Jatropha MQL surpassed jatropha emulsion, mineral emulsion, and mineral MQL by 75.8%, 81.2%, and 90.5%, respectively.

- The noise performance of jatropha MQL exceeded jatropha oil emulsion, mineral oil emulsion, and mineral MQL by 9.2%, 7.2%, and 13.9%, respectively.
- Spindle speed is the most important variable influencing machine vibration and sound level, according to the analysis of variance.
- For machine sound and vibration, the optimum spindle speed, feed rate, and depth of cut were 355 rev/min, 0.10 mm/rev, and 0.75 mm, and 355 rev/min, 0.15 mm/rev, and 1.00 mm, respectively.

Fig. 41 Surface plot of SS, DOC, and MSL for mineral oil emulsion
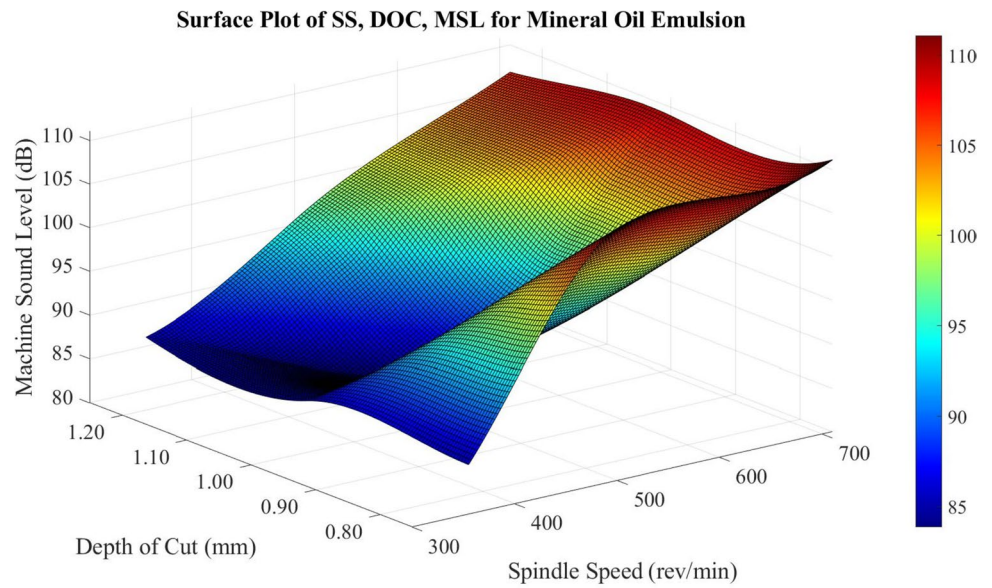
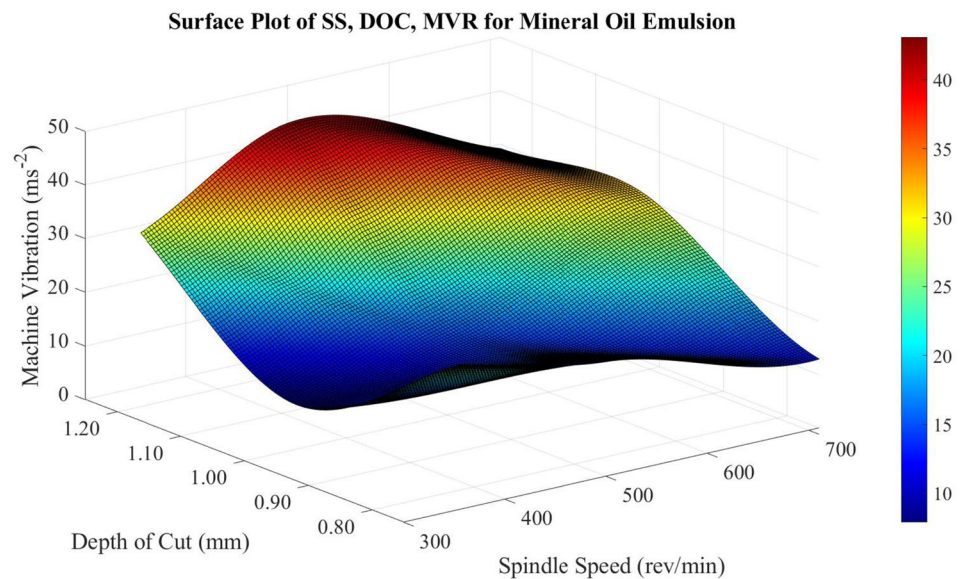**Fig. 42** Contour plot of SS, DOC, and MVR for mineral oil emulsion
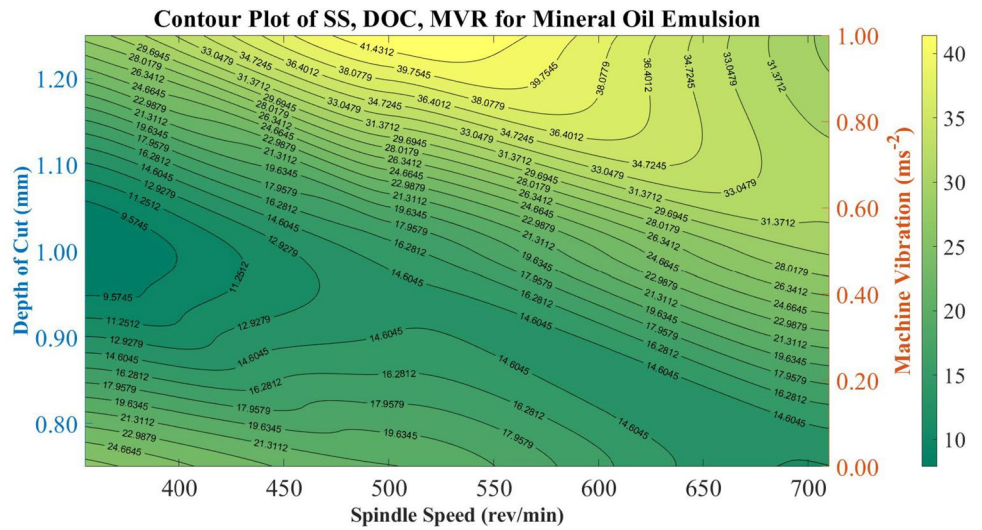
5 Recommendation

Based on the findings of a turning test on AISI 1525 steel with a tungsten carbide tool and two distinct oils—mineral oil and watermelon oil—as cutting fluids, this study offers the following recommendations.

- Further tests should be carried out, perhaps using the Taguchi L27 orthogonal array to quantify the statistical analysis, for a more thorough examination.
- Further studies could involve the inclusion of nanoparticles to watermelon oil.

Fig. 43 Surface plot of SS, DOC, and MVR for mineral oil emulsion

- The MQL flow rate could be considered as a factor in subsequent research.

Declarations

References

1. Abegunde PO, Kazeem RA, Akande IG, Ikumapayi OM, Adebayo AS, Jen TC, Akinlabi SA, Akinlabi ET (2023) Performance assessment of some selected vegetable oils as lubricants in turning of AISI 1045 steel using a Taguchi-based grey relational analysis approach. Tribol Mater Surf Interf 17(3):187–202
2. Agastra E, Pelosi G, Selleri S, Taddei R (2013) Taguchi's method for multi-objective optimization problems. Int J RF Microwave Comput Aided Eng 23(3):357–366
3. Akkuş H, Yaka H (2021) Optimization of cutting parameters in turning of titanium alloy (grade 5) by analysing surface roughness, tool wear and energy consumption. Exp Tech 46:945–956
4. Alaba ES, Kazeem RA, Adebayo AS, Petinrin MO, Ikumapayi OM, Jen TC, Akinlabi ET (2023) Evaluation of palm kernel oil as cutting lubricant in turning AISI 1039 steel using Taguchi-grey relational analysis optimization technique. Adv Ind Manuf Eng 6:100115
5. AOAC (1975) Official methods of analysis. AOAC International, Washington, DC
6. Bhogal, S. S., Sindhu, C., Dhami, S. S., & Pabla, B. S. (2015). Minimization of surface roughness and tool vibration in CNC milling operation. *J Optim*, *2015*.
7. Bhuiyan MSH, Choudhury IA (2015) Investigation of tool wear and surface finish by analyzing vibration signals in turning Assab-705 steel. Mach Sci Technol 19(2):236–261
8. Capdevila M, Maestro A, Porras M, Gutiérrez JM (2010) Preparation of Span 80/oil/water highly concentrated emulsions: Influence of composition and formation variables and scale-up. J Colloid Interface Sci 345(1):27–33
9. Chuangwen X, Jianming D, Yuzhen C, Huaiyuan L, Zhicheng S, Jing X (2018) The relationships between cutting parameters, tool wear, cutting force and vibration. Adv Mech Eng 10(1):1687814017750434
10. Deshpande Y, Andhare A, Sahu NK (2017) Estimation of surface roughness using cutting parameters, force, sound, and vibration in turning of Inconel 718. J Braz Soc Mech Sci Eng 39:5087–5096
11. D'Mello G, Pai PS, Puneet NP, Fang N (2016) Surface roughness evaluation using cutting vibrations in high speed turning of

Ti-6Al-4V-an experimental approach. Int J Mach Mach Mater 18(3):288–312

12. Duan Z, Li C, Zhang Y, Yang M, Gao T, Liu X, Li R, Said Z, Debnath S, Sharma S (2023) Mechanical behavior and Semiempirical force model of aerospace aluminum alloy milling using nano biological lubricant. Front Mech Eng 18(1):4

13. Duan Z, Yin Q, Li C, Dong L, Bai X, Zhang Y, Yang M, Jia D, Li R, Liu Z (2020) Milling force and surface morphology of 45 steel under different Al 2 O 3 nanofluid concentrations. Int J Adv Manuf Technol 107:1277–1296

14. Flinders M, Ray D, Anderson A, Cutler RA (2005) High-toughness silicon carbide as armor. J Am Ceram Soc 88(8):2217–2226

15. Ghani AK, Choudhury IA (2002) Study of tool life, surface roughness and vibration in machining nodular cast iron with ceramic tool. J Mater Process Technol 127(1):17–22

16. Ghorbani S, Kopilov VV, Polushin NI, Rogov VA (2018) Experimental and analytical research on relationship between tool life and vibration in cutting process. Archiv Civil Mech Eng 18:844–862

17. Ghosh PS, Chakraborty S, Biswas AR, Mandal NK (2018) Empirical modelling and optimization of temperature and machine vibration in CNC hard turning. Mater Today Proc 5(5):12394–12402

18. Jonas M, Ketlogetswe C, Gandure J (2020) Variation of Jatropha curcas seed oil content and fatty acid composition with fruit maturity stage. Heliyon 6(1):e03285

19. Kam M, Şeremet M (2021) Experimental and statistical investigation of surface roughness and vibration during finish turning of AISI 4140 steel workpiece under cooling method. Surf Rev Lett 28(10):2150092

20. Kazeem RA, Fadare DA, Abutu J, Lawal SA, Adesina OS (2020) Performance evaluation of jatropha oil-based cutting fluid in turning AISI 1525 steel alloy. CIRP J Manuf Sci Technol 31:418–430

21. Kazeem RA, Fadare DA, Akande IG, Jen TC, Akinlabi SA, Akinlabi ET (2024) Evaluation of crude watermelon oil as lubricant in cylindrical turning of AISI 1525 steel employing Taguchi and grey relational analyses techniques. Heliyon 10(3):e25349

22. Kazeem RA, Fadare DA, Ikumapayi OM, Azeez TM, Adediran AA (2022) Development of bio-cutting fluid (cirtullus lanatus) and its performance assessment on the machining of AISI 1525 steel using Taguchi technique and grey relational analysis. Biointerface Res Appl Chem 12(4):5324–5346

23. Koushki A, Jalali A, Rasooli N, Heydarinia A, Geranmayeh A, Mehranpour MS, Shahmir H (2024) Strength-ductility synergy in a wrought AZ80 magnesium alloy by microstructure engineering. Mater Sci Eng, A 889:145764

24. Lawal SA, Choudhury IA, Nukman Y (2014) Evaluation of vegetable and mineral oil-in-water emulsion cutting fluids in turning AISI 4340 steel with coated carbide tools. J Clean Prod 66:610–618

25. Lee WC, Wei CC, Chung SC (2014) Development of a hybrid rapid prototyping system using low-cost fused deposition modeling and five-axis machining. J Mater Process Technol 214(11):2366–2374

26. Liang SY (2019) Subtractive processes—traditional operations: cutting, grinding, and machine tools. In: Handbook of manufacturing. World Scientific, p 17

27. Luo H, Wang X, Liu Z, Yang Z (2020) Influence of refined hierarchical martensitic microstructures on yield strength and impact toughness of ultra-high strength stainless steel. J Mater Sci Technol 51:130–136

28. Mohanta RK, Chelliah TR, Allamsetty S, Akula A, Ghosh R (2017) Sources of vibration and their treatment in hydro power stations-A review. Eng Sci Technol Int J 20(2):637–648

29. Muniz CAS, Dantas TNC, Moura EF, Neto AD, Gurgel A (2009) Novel formulations of cutting fluids using naphtenic basic oil. Braz J Pet Gas 2(4):143–153

30. Orhan S, Er AO, Camuşcu N, Aslan E (2007) Tool wear evaluation by vibration analysis during end milling of AISI D3 cold work tool steel with 35 HRC hardness. NDT and E Int 40(2):121–126

31. Özbek O, Saruhan H (2020) The effect of vibration and cutting zone temperature on surface roughness and tool wear in ecofriendly MQL turning of AISI D2. J Market Res 9(3):2762–2772

32. Quintana G, Ciurana J (2011) Chatter in machining processes: A review. Int J Mach Tools Manuf 51(5):363–376

33. Rafighi M (2022) Effects of shallow cryogenic treatment on surface characteristics and machinability factors in hard turning of AISI 4140 steel. Proc Inst Mech Eng Part E J Proc Mech Eng 236(5):2118–2130

34. Rafighi M (2022) The cutting sound effect on the power consumption, surface roughness, and machining force in dry turning of Ti-6Al-4V titanium alloy. Proc Inst Mech Eng C J Mech Eng Sci 236(6):3041–3057

35. Rao KV, Kumar YP, Singh VK, Raju LS, Ranganayakulu J (2021) Vibration-based tool condition monitoring in milling of Ti-6Al-4V using an optimization model of GM (1, N) and SVM. Int J Adv Manuf Technol 115(5–6):1931–1941

36. Rao KV, Murthy BSN, Rao NM (2014) Prediction of cutting tool wear, surface roughness and vibration of work piece in boring of AISI 316 steel with artificial neural network. Measurement 51:63–70

37. Risbood KA, Dixit US, Sahasrabudhe AD (2003) Prediction of surface roughness and dimensional deviation by measuring cutting forces and vibrations in turning process. J Mater Process Technol 132(1–3):203–214

38. Şahinoğlu A, Rafighi M (2020) Investigation of vibration, sound intensity, machine current and surface roughness values of AISI 4140 during machining on the lathe. Arab J Sci Eng 45:765–778

39. ŞahinoğluGüllü Ciftci AAI (2019) Analysis of surface roughness, sound level, vibration and current when machining AISI 1040 steel. Sigma J Eng Nat Sci 37(2):423–437

40. Sani ASA, Abd Rahim E, Sharif S, Sasahara H (2019) The influence of modified vegetable oils on tool failure mode and wear mechanisms when turning AISI 1045. Tribol Int 129:347–362

41. Sarma DK, Dixit US (2007) A comparison of dry and air-cooled turning of grey cast iron with mixed oxide ceramic tool. J Mater Process Technol 190(1–3):160–172

42. Sen B, Gupta MK, Mia M, Pimenov DY, Mikołajczyk T (2021) Performance assessment of minimum quantity castor-palm oil mixtures in hard-milling operation. Materials 14(1):198

43. Siddhpura M, Paurobally R (2012) A review of chatter vibration research in turning. Int J Mach Tools Manuf 61:27–47

44. Swain S, Panigrahi I, Sahoo AK, Panda A, Kumar R (2020) Effect of tool vibration on flank wear and surface roughness during high-speed machining of 1040 steel. J Fail Anal Prev 20(3):976–994

45. Vasanth XA, Paul PS, Lawrance G, Varadarajan AS (2019) Vibration control techniques during turning process: a review. Aust J Mech Eng

46. Venkata Rao K, Murthy PBGSN (2018) Modeling and optimization of tool vibration and surface roughness in boring of steel using RSM, ANN and SVM. J Intell Manuf 29(7):1533–1543

47. Wegener K, Bleicher F, Heisel U, Hoffmeister HW, Moehring HC (2021) Noise and vibrations in machine tools. CIRP Ann 70(2):611–633

48. Wei W, Shang Y, Peng Y, Cong R (2022) Research progress of noise in high-speed cutting machining. Sensors 22(10):3851

49. Yan Z, Zhu J, Zhang Z, Wang Q, Xue Y (2022) The microstructural, textural, and mechanical effects of high-pressure torsion processing on Mg alloys: A review. Front Mater 9:964992

50. Yang CAO, Yejun ZHU, Wenfeng DING, Yutong QIU, Lifeng WANG, Jiuhua XU (2022) Vibration coupling effects and machining behavior of ultrasonic vibration plate device for creep-feed grinding of Inconel 718 nickel-based superalloy. Chin J Aeronaut 35(2):332–345

51. Yi S, Li J, Zhu J, Wang X, Mo J, Ding S (2020) Investigation of machining Ti-6Al-4V with graphene oxide nanofluids: tool wear, cutting forces and cutting vibration. J Manuf Process 49:35–49

52. Zhenjing D, Changhe L, Zhang Y, Lan D, Xiufang B, Min Y, Jia D, Cao LR, H, Xuefeng, X, (2021) Milling surface roughness for 7050 aluminum alloy cavity influenced by nozzle position of nanofluid minimum quantity lubrication. Chinese J Aeronaut 34(6):33–53

53. Zhou X, Tan W, Sun Y, Huang T, Yang C (2024) Multi-objective optimization and decision making for integrated energy system using STA and fuzzy TOPSIS. Expert Syst Appl 240:122539